CHEMISTRY
A European Journal

A Journal of
ChemPubSoc Europe

Accepted Article

Title: Modulation of Antimalarial Activity at a Putative Bisquinoline Receptor in vivo Using Fluorinated Bisquinolines

Authors: Alistar John Fielding, Valentina Lukinovic, Philip Evans, said Alizadeh, Roger Bisby, Mike Drew, ALESSIO DEL CASINO, James Dunn, Laura Randle, Nicola Dempster, Nahar Lutfun, Sarker Satyajit, Fabián G. Cantú Reinhard, Sam P. de Visser, Mike Dascombe, and Fyaz Ismail

To be cited as: *Chem. Eur. J.* 10.1002/chem.201605099

Link to VoR: http://dx.doi.org/10.1002/chem.201605099

Supported by
ACES

WILEY-VCH

10.1002/chem.201605099

Modulation of Antimalarial Activity at a Putative Bisquinoline Receptor *in vivo* Using Fluorinated Bisquinolines

Alistair J. Fielding [a]*, Valentina Luković [a], Philip G. Evans [b], Said Alizadeh-Shekalgourabi [c], Roger H. Bisby [d], Michael G. B. Drew [e], Alessio Del Casino [f], James F. Dunn [f], Laura E. Randle [f], Nicola M. Dempster [f], Lutfun Nahar [f], Satyajit D. Sarker [f], Fabián G. Cantú Reinhard [g], Sam P. de Visser [g], Mike J. Dascombe [h], Fyaz M. D. Ismail [f]*

[a]School of Chemistry and the Photon Science Institute, The University of Manchester, Manchester M13 9PL, United Kingdom.

[b]Peakdale Molecular Limited, Discovery Park, Sandwich, Kent, CT13 9FF, United Kingdom.

[c]Department of Pharmacy, University of Hertfordshire, Hatfield, Hertfordshire, AL10 9AB, , United Kingdom.

[d]Biomedical Sciences Research Institute, University of Salford, Salford M5 4WT, United Kingdom.

[e]School of Chemistry, The University of Reading, Whiteknights, Reading RG6 6AD, United Kingdom.

[f]Medicinal Chemistry and Natural Products Research Group, School of Pharmacy and Biomolecular Sciences, Liverpool John Moores University, Byrom Street, Liverpool L3 3AF, United Kingdom.

[g]Manchester Institute of Biotechnology, School of Chemical Engineering and Analytical Science, The University of Manchester, 131 Princess Street, Manchester, M1 7DN, United Kingdom.

[h]Faculty of Biology, Medicine and Health, Stopford Building 1.124, The University of Manchester, Oxford Road, Manchester M13 9PT, United Kingdom.

10.1002/chem.201605099

Abstract

Antimalarials can interact with heme covalently, by π-π interactions or hydrogen bonding. Consequently, the prototropy of 4-aminoquinolines and quinoline methanols was investigated using quantum mechanics. Calculations showed mefloquine protonated preferentially at the piperidine and was impeded at the endocyclic nitrogen due to electronic rather than steric factors. In gas phase calculations, 7-substituted *mono*- and *bis*-4-aminoquinolines were preferentially protonated at the endocyclic quinoline nitrogen. By contrast, compounds with a trifluoromethyl substituent on both the 2- and 8-positions, reversed the order of protonation which now favored the exocyclic secondary amine nitrogen at the 4-position. Loss of antimalarial efficacy by CF_3 groups simultaneously occupying the 2- and 8-positions was recovered if the CF_3 group occupied the 7-position. Hence, trifluromethyl groups buttressing quinolinyl nitrogen shifted binding of antimalarials to hematin, enabling switching from endocyclic to the exocyclic N. Both theoretical calculations (DFT calculations: B3LYP/6-31+G*) and crystal structure of (±)-*trans*-N^1,N^2-*bis*-(2,8-ditrifluoromethylquinolin-4-yl)cyclohexane-1,2-diamine were used to reveal preferred mode(s) of interaction with hematin. The order of antimalarial activity *in vivo* followed the capacity for a redox change of the iron(III)state which has important implications for the future rational design of 4-aminoquinoline antimalarials.

KEYWORDS: trifluorinated antimalarials, drug-receptor, pharmacology, X-ray crystallography, DFT modelling, bisquinolines, NMR, EPR

Introduction

It is unlikely that an effective and affordable antimalarial vaccine will become available in the near future for widespread use; therefore, antimalarial drugs will continue to be important in the management and treatment of malaria. One currently effective, but expensive, antimalarial drug is the fluorinated quinoline methanol, mefloquine **1** [Lariam^{TM}, (*R, S)*-(±)-α-2-piperidinyl-2,8-(*bis*-trifluoromethyl)-4-quinolinyl methanol]. Despite limited clinical use, the incidence of drug resistance to **1a** continues to increase worldwide. Also of great concern, especially to travelers from wealthy non-endemic countries, is the occurrence of adverse neuropsychiatric reactions to **1a**.[1] It is imperative, therefore, to construct congeners of existing antimalarials, as well as identifying new drug leads in order to provide a range of selectively toxic, clinically useful antimalarial agents and to determine the molecular mechanism(s) of antimalarial action. Our research in this area has led to the characterization of a putative bisquinoline receptor encoded with desirable features within 4-aminoquinolines and, perhaps, quinoline methanol antimalarials with activity *in vivo*.[2]

Certain biochemical and pharmacological evidence suggests that 4-aminoquinolines such as **5** interfere with heme processing[3] although this hypothesis has been challenged.[4] The poor solubility of these bisquinolines in common solvents necessitated use of theoretical methods in order to predict sites of protonation and lipophilicity. Despite the exact molecular sequence of events that lead to *Plasmodial* death not being known, it is currently accepted that processes leading up to and involving the formation of hemozoin *(β*-hematin)[i] can be

[i]Four ferrous-protoporphyrin IX molecules, prosthetic adducts of hemoglobin, are enzymatically catabolized per molecule of hemoglobin by parasites. Fe(II)PPIX is oxidized to form Fe(III)PPIX and is denoted hematin (α-hematin), and possesses an axial OH substituent. Following biomineralisation, it is chemically identical to *β*-hematin (synthetic) known as hemozoin. In this biomineral, coordination of the central iron atom of one molecule to one carboxyl of the adjacent molecule forms a reciprocal dimer (rather than an infinite polymer). Synthetic *β*-hematin obtained chemically in acidic conditions *in vitro* appears identical to physical and spectroscopic characteristics of native, parasite produced pigment. [5]

disrupted *in vitro* by 4-aminoquinolines[6] and quinoline methanols.[3c]

The absence of fluorine in mammalian systems as well as the high natural abundance of this NMR active isotope (^{19}F)[7] has been previously exploited as a sensitive probe for quinoline receptor binding in solution.[8] Fluorine remains a popular choice for modifying leads inspired by natural products into useful drugs.[9]

Cartographic analysis[10] based on mass spectroscopy of **1** distribution within *Plasmodia* has revealed its accumulation profile.[11] Interestingly, when first tested, Andersag *et al* [12] found that the trifluoromethyl bioisostere **4b** of chloroquine **4a** failed to confer advantages of incorporating fluorine in a molecule. Subsequently, this compound has been reconsidered as a useful compound for evaluating its antiparasitic activity *in vivo*; a result subsequently confirmed[13] against both sensitive and resistant strains *in vitro*.

Van der Werf *et al*.[14] pioneered bioisosteric replacement of the hydroxyl group of amodiaquine **8a** with fluorine, which resulted in less activity than **8a** *in vivo*.[15] Although, this known compound also showed a corresponding loss of antimalarial potency when compared to amodiaquine *in vitro*, the need for new antimalarials was such that it was successfully patented much later.[16] A greater degree of success has been achieved in the 8-aminoquinoline class of compounds, such as WR 238, 605 (Tafenoquine **9**), which benefit from judicious introduction of trifluoromethyl substituents into the side chain.[17] From the latter half of the twentieth century, impact on metabolism by the host has become an important regulatory factor and fluorine now occurs in almost ~20 % of new drug introductions.[9]

The synthesis and pharmacological profile of **1** resulted from the antimalarial program initiated by the US Army during World War II; the drug came into use after the end of the

US-Vietnam conflict.[18] A mefloquine progenitor, **2** was first disclosed in a comprehensive survey of antimalarials by Wiselogle,[18f] which also showed that in quinine **3** the quinuclidine ring could be simplified. They also showed that the methoxy group could be replaced by halogens (concurrently enhancing overall drug lipophilicity) resulting in 80 times greater activity than **3**, initially in a duck (*Plasmodium cathemerium*)[18c] and subsequently in a murine model of malaria (*Plasmodium berghei*).[4b, 18g, 18h] Introduction of the lipophilic groups into position 2 of both **1** and **2** effectively delayed premature metabolic inactivation at this position by oxidation, an assumed weakness of **3**.[19] Unfortunately, the prolonged photosensitizing action of **2** prevented further development of this *seco*-derivative into a clinically useful drug.[4b, 18h] By contrast, the introduction of trifluoromethyl (CF_3) groups into positions 2 and 8 was dictated by bioassay-guided antimalarial screening. This provided a compound with an improved antimalarial/pharmacological profile against *Plasmodium berghei in vivo*.[18b, 18c] Similarly, the exact role of substituent positioning, especially chlorine on position 7 in 4-aminoquinoline antimalarials (Figure 1, **4a**; **5**) has never been adequately clarified. Presumably the chlorine groups in **5** impart improved lipophilic and/or pharmacokinetic properties, but they may also serve a yet undefined pharmacodynamic role. Studies of chloro and *des*-chloro analogs in a heme binding assay suggest that this group in the 7-position enhances binding of chloroquine-like drugs to the putative monomeric heme drug target[20] or interpenetrating a heme μ-oxo dimer.[21] The structural significance of halogenated substituents remains unknown but can certainly modulate metabolism in both parasite and host by "halogen blocking" receptors.[22]

10.1002/chem.201605099

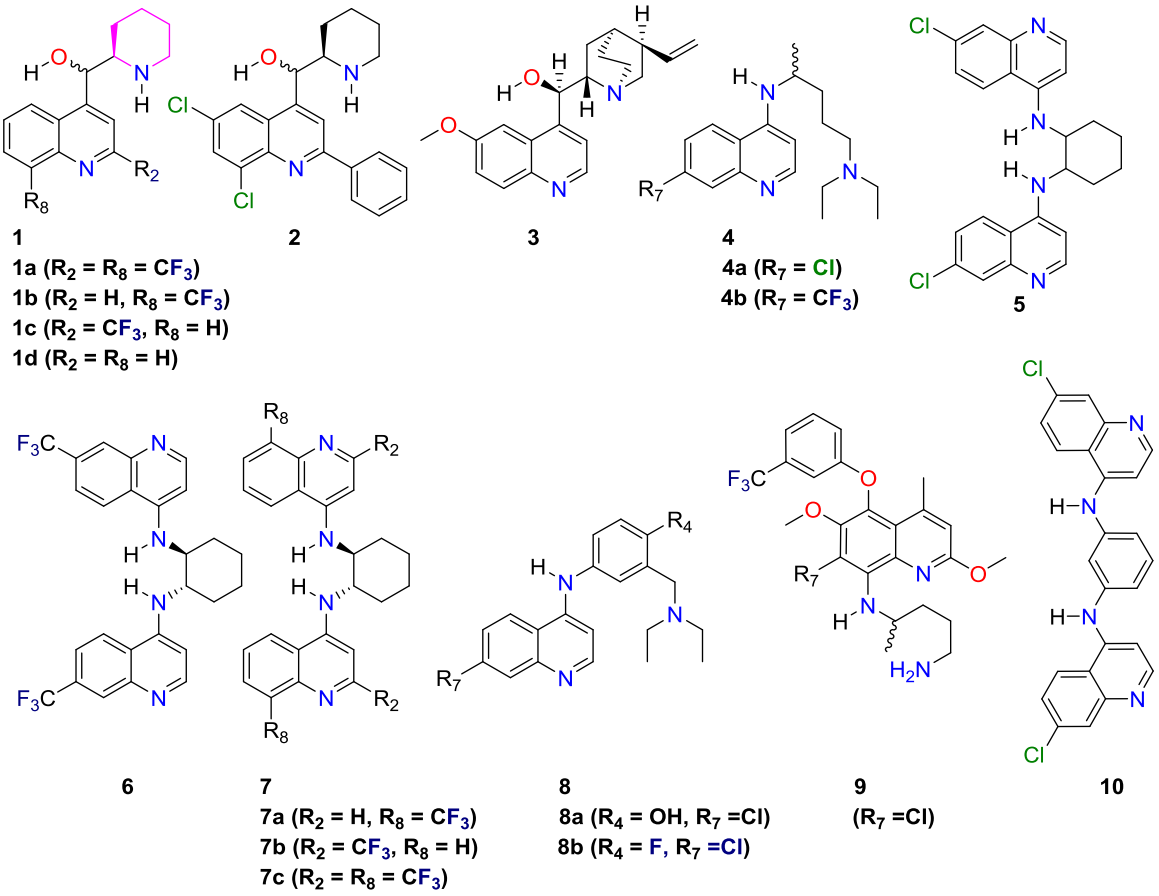

Figure 1. Structural formulae of known and novel antimalarials described in this study, wherein **1a** represents mefloquine (cycloaliphatic piperidinyl ring highlighted in magenta), **2** (6, 8-Dichloro-2-phenyl-quinolin-4-yl)-piperidin-2-yl-methanol, **3** quinine, **4a** chloroquine. **5**, **6**, **7** without additional letters are used generically to describe any isomer. There are two isomers for these three compounds named as -*trans* (R-R) with *trans* geometry, and -*cis* (R,S) with *cis* geometry, with the identifiers equatorial (eq) and axial (ax), respectively, referring to the position of the substituent amino nitrogen atoms relative to the cyclohexane ring. **8a** represents amodiaquine, **9** WR 238,605 (Tafenoquine) [17] and **10** metaquine.[23]

One enantiomer of **4** demonstrated greater antimalarial efficacy than the other.[24] Similarly, enantiomers of **1a** possess differing pharmacodynamic and pharmacokinetic profiles.[25] Potent compounds developed using a putative antimalarial receptor model include

individual enantiomers of (±)-*trans*-N^1,N^2-*bis*-(7-chloroquinolin-4-yl)cyclohexane-1,2-diamine (**5**-*trans*, ID_{50} < 2.5 mg/kg, 5.7 mmol/kg) as well as its structural isomer **5**-*cis* see Figure 1).[2]

In 1998, Ismail *et al*. reported a molecular mechanics study detailing the range of binding geometries of metaquine (**10**, Figure 1) to hematin.[26] In this report, a number of close contacts with the receptor[22] were revealed, involving hydrogen bonds. Such observations, prompted the construction of a lead compound incorporating bulky CF_3 groups[7, 27] in positions 2 and 8 of the quinoline ring and bridged at position 4 with (±)-*trans*-1,2-diaminocyclohexane to make a *bis*-(mefloquine/4-aminoquinoline) hybrid. In addition, one or more suitably positioned CF_3 groups were expected to modulate, either favorably or unfavorably, lipophilicity[7, 28] as well as protect various antimalarials from xenobiotic metabolism.[7, 29]

In order to further refine a generalized receptor model[23] in this current investigation, we examined factors modulating antimalarial activity and explored possible homology with mefloquine-type compounds. A mefloquine/bisquinoline hybrid was constructed to ascertain what effect this would have on antimalarial activity *in vivo* and (i) to elucidate hydrogen bonding sites within these drugs and the influence of CF_3 substituents; (ii) to explore the potential sites of protonation through quantum mechanical calculations[23] and (iii) to examine these interactions using X-ray crystallography and extensive DFT calculations involving interactions of various ligands with heme.

Results and discussion

Synthesis

Compounds **5** and **6** were constructed using anhydrous NMP/triethylamine as reported previously.[2] The target substance (±)-*trans*- N^1,N^2-*bis*-(2,8-ditrifluoromethyl-quinolin-4-yl)

10.1002/chem.201605099

cyclo-hexane-1, 2-diamine **7c** was constructed by refluxing freshly distilled (±)-*trans*-1,2-diaminocyclohexane with two equivalents of the corresponding 4-halo-2,8-*bis*-trifluoromethyl substituted quinolines under a blanket of argon. Use of anhydrous *N*-methylpyrollidinone (NMP)/ triethylamine under reflux encouraged dimer formation **7c** [2] (Figure 2).

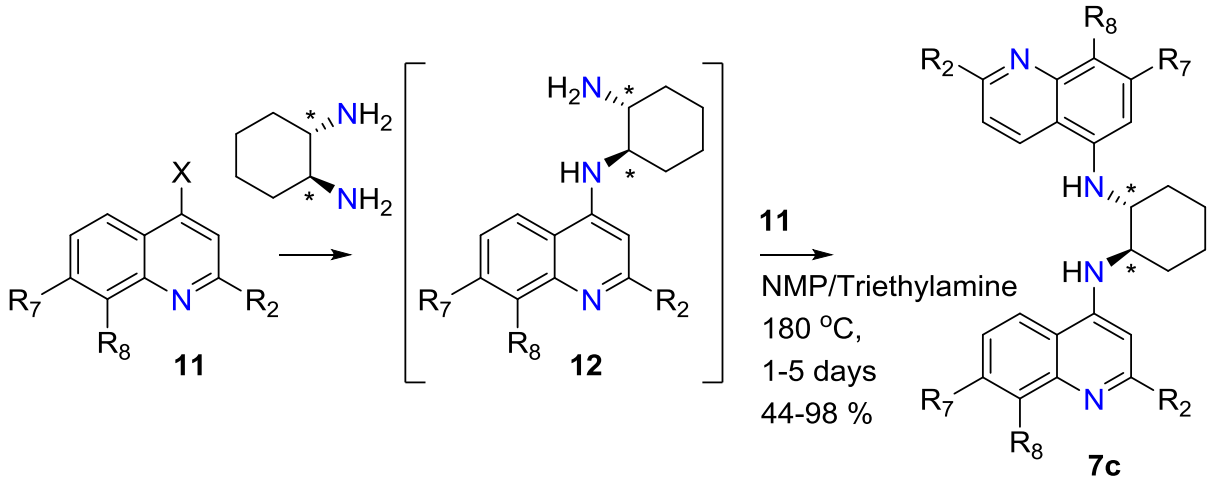

Figure 2. Stepwise *de*-halogenoamination with S_NAr reaction illustrating *mono*- and *bis*-quinoline formation where (R_2 = H or CF_3; R_7 = Cl or H, or various combinations thereof; R_8 = H or CF_3).

When 4-bromo (or 4-chloro)-2,8-trifluormethylquinoline was used for the S_NAr (aromatic nucleophilic substitution) reaction, the reaction mixtures always became blue-black despite the presence of a protective atmosphere of argon. It is possible that the reactants or products were photosensitive, hence all further experiments were conducted in aluminum foil covered reactors. Both 4-chloro- and 4-bromo-2,-8-(*bis*-trifluoromethyl)-quinoline reacted with (±)-*trans*-1,2-diaminocyclohexane triethylamine/NMP (180 °C, 5 days, sand bath) to provide the required product **7c** in 88 % crude yield.[2] Repeated recrystallization of the crude brown/black reaction mixture from acetone/HCl gave analytically pure **7a** (44 % yield). The

(±)-*trans*-N^1-(2,8-di-trifluoromethylquinolin-4-yl) cyclohexane-1,2-diamine intermediate **12** (Figure 2) was detected by spectrometry as an intermediate. The poor solubility profile, typical of such salts e.g. **5**, [2] prevented the acquisition of NMR spectra of the salt necessitating conversion to the free base for such experiments. Nevertheless, the solubility of **7c** in DMSO was still inadequate, necessitating long spectral acquisition times and the use of a probe optimized for ^{13}C HMBC and HSQC. A convenient, focused microwave preparation unlike the thermal synthesis, formed fewer dark by-products, is given in the Supporting Information.

EI-MS spectra (m/z = 640 Da) revealed loss of a fluorine radical from the mass ion leading onto complex fragmentation and rearrangement phenomena (not shown). Since the base ion was m/z = 36 (with the expected chlorine isotope patterns), this verified the (unexpected) presence of **7c** as a hydrochloride salt. Additional evidence from both nominal and accurate positive ion high resolution electrospray ionization-mass spectrometry of the free base confirmed the identity of the compounds (see Supporting Information).

HPLC analysis showed monomeric impurities such as **11** were absent in the purified compounds used in the studies reported here. Positive-ion HR-ESI-MS was performed to confirm whether compounds **6**-*trans* and **7c**-*trans* were singly or doubly protonated (Supporting Information). Results indicated that both compounds were exclusively mono-protonated. The resultant accurate mass positive ion spectra indicate good agreement between predicted and observed mass spectra (Table 1 and Supporting Information).

Only the 4-aminoquinoline compounds **5** and **6** formed strong complexes with heme in electrospray experiments using methanol as the solvent (see Supporting Information). The interactions with heme of both **6**-*trans* and **7c**-*trans* as well as their protonated species, were studied further using molecular modeling methods (see below).

Spectroscopic Studies

The state of ionization of antimalarial drugs is influenced by the environmental pH for example whether or not the drug is in the acidic digestive vacuole of *Plasmodium*. In order to determine the effect of protonation on **6**-*trans* and **7c**-*trans* the UV spectra were determined in DMSO and in trifluoroacetic acid (TFA). The compounds exhibited similar UV spectra with two-three maxima in DMSO and TFA (Table 2 and Figure S17) with chromic shifts reflecting conformational changes upon protonation which were subsequently investigated using quantum mechanics. Protonation of 6-*trans* in DMSO results in a reduction of basicity which caused a hyposchromic shift of a π to π^* band in TFA whereas the opposite was noted for **7c**-*trans* (bathochromic shift). These observations are consistent with previous studies on related heterocyclic compounds, in which a hypsochromic shift has been related to protonation at the endocyclic nitrogen whereas bathochromic shift is associated with protonation at the exocyclic nitrogen.[30] Protonation of the endocyclic nitrogen changes the effective electronegativity of this position, the change in the charge on the nitrogen atom upon excitation determines the magnitude of the bathochromic spectral shift upon protonation (or deprotonation of the cation).[31] The increase in extinction coefficients of **7c**-*trans* from moving to an increased hydrogen bonding environment reflects the geometrical change involved on the torsion angles upon protonation and its subsequent interaction on the chromophore. In the case of **6**-*trans,* the corresponding increase of the extinction coefficients from a slightly basic (DMSO) to an acidic medium reflects the change in geometry on protonation of the endocyclic nitrogen at position 1 as well as hydrogen bonding of the endocyclic nitrogen that is known to add as a proton donor. In both **6**-*trans* and **7c**-*trans* the change from a basic to hydrogen bonding solvent increases the extinction coefficients as expected. These results are consistent with arguments advanced by Ganguly and Banerjee involving secondary amines.[32] The shifts in the UV spectra could therefore be used to establish both the state of protonation and determine intra-cellular trafficking in *vitro*.

Table 1. Observed and predicted masses for **6**-*trans* and **7c**-*trans*.

COMPOUND	PREDICTED	OBSERVED	DISCREPANCY
6-*trans*	505.1821	505.1805	3 ppm
7c-*trans*	641.1575	641.1491	13 ppm

Table 2. UV-spectroscopic data for **6**-*trans* and **7c**-*trans* indicating chromic shifts upon ionization.

Compound	Solvent	Bands
6-*trans*	DMSO	337 nm ($\varepsilon \sim$ 24,138)
		351 nm ($\varepsilon \sim$ 26,601)
6-*trans*	TFA	328 nm ($\varepsilon \sim$ 40,367)
		342 nm ($\varepsilon \sim$ 46,789)
7c-*trans*	DMSO	354 nm ($\varepsilon \sim$ 21,675)[i]
7c-*trans*	TFA	338 nm ($\varepsilon \sim$ 37,615)
		344 nm ($\varepsilon \sim$ 40,367)
		362 nm ($\varepsilon \sim$ 55,963)

[i]Broad band.

NMR experiments

The projected receptor binding experiments require unequivocal identification of both quaternary centers associated with the trifluoromethyl group, because they could be sensitive probes for the drug-binding environment. Hence, both trifluoromethyl groups were identified by the magnitude of the $^{1}J_{C\text{-}F}$ and $^{2}J_{C\text{-}F}$ coupling constants. Partial analysis of vicinal coupling constants ascribed to the (±)-*trans*-1,2-diamino-cyclohexane bridging unit suggests that the

10.1002/chem.201605099

axial-axial conformer predominates in DMSO-d_6 solution, at room temperature, an observation consistent with the solid state structure (see Figure 7). The latter reveals the desired position of hydrogen bonding, the NH proton being split into a doublet by one of two of the eight protons found in this complex, a result confirmed by COSY experiments (Figure 3). This condition remained unchanged in the presence of both strongly and weakly coordinating solvents such as NMP and methanol. The result confirms that the exocyclic secondary amino group participates in hydrogen bonding interactions confirming its role as a donor group and probably acts with heme in a similar fashion (See modeling section).[2, 23]

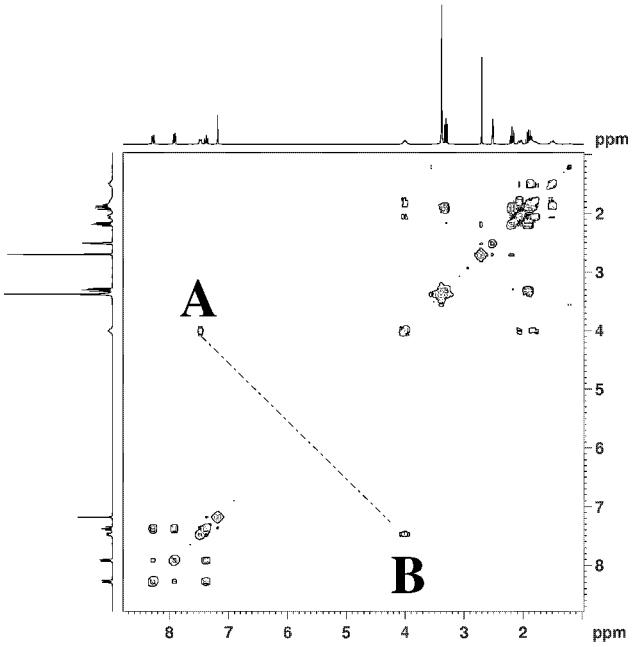

Figure 3. COSY spectrum of **7c**-*trans*. Marked is the cross peak between NH at **A** and a molecule of water at **B**.

Pharmacology

Compound **7c** injected subcutaneously (s.c.) twice daily in mice infected with chloroquine-sensitive *P. berghei*[2] (dose levels 10 and 50 mg/kg, 23.6 and 117.8 mmol/kg respectively; n = 5) had no effect on parasitaemia 72 hours after inoculation with *Plasmodium*, when compared with vehicle-treated animals (control 64.8 ± s.e.m. 2.1 %, **7c** 10

mg/kg (23.6 mmol/kg) 61.6 ± 1.55 %, **7c** 50 mg/kg (117.8 µmol/kg) 66.1 ± 2.7 % erythrocytes contained Leishman-positive bodies, $P > 0.05$, Mann-Whitney U). Repeated administration of **7c** in these doses over the three day period was also without effect on body weight gain, colonic temperature, locomotor activity or, by visual inspection, the general autonomic state of mice when compared with control animals receiving vehicle (olive oil/DMSO 24:1, injection volume 10 ml/kg s.c.). In contrast, **6** tested in this murine model of malaria was antimalarial (ID_{50} 5.9 mg/kg; 14.9 µmol/kg). Previously, we have tested **6** [2a] and found it to have less antimalarial activity than the two configurations of **5**,[2a] suggesting its interaction with the target receptor is sterically unfavorable. A similar loss of antimalarial potency in the trifluromethyl analog of chloroquine may explain why it was not developed further.[33] Compound **6** injected s.c. in mice infected with *P. berghei* (dose range 6.3-252.2 µmol/kg, 5 doses in 72 hours) produced no observable adverse effects. Chloroquine diphosphate in this model had an ID_{50} of 4.3 mg/kg (8.3 µmol/kg).

Comparison of the data for putative 4-aminoquinoline antimalarials containing CF_3 groups in both the 2- and 8- positions, indicates that they all showed decreased antimalarial activity compared to their 7- CF_3 counterparts either *in vitro* or *in vivo*. [13-16, 34]

Theoretical Investigations: Comparison of quinoline methanol behavior versus 4-aminoquinolines.

Conformational analyses were carried out on mefloquine **1** and its progenitor **2**. A comparison of the crystal structures of different forms of mefloquine, namely (±) mefloquine methylsulfonate monohydrate, (±) mefloquine hydrochloride methanol solvate,[35] (±) mefloquine free base, and (-) mefloquine hydrochloride hydrate,[36] shows that all four structures contain short N...O contacts of 2.73-2.94 Å, with a geometry similar to that shown in Figure 4, which can be considered as hydrogen bond interactions.

10.1002/chem.201605099

Conformational analysis on **1a** using molecular dynamics was undertaken. The simulations were carried out at 3000 K with step sizes of 1 fs. 1000 structures were saved at 1 ps intervals and geometry optimized by molecular mechanics using the Dreiding force field within Cerius^2. [37] Two low energy conformations were obtained in this study, which differed only in the O-C-C-N torsion angle. These were subsequently geometry optimized using the Gaussian09 program[38] with DFT at the B3LYP/6-31+G* level of theory: the structure which contained a torsion angle of -68.2^o with a hydrogen bond had a lower energy by 4.5 kcal mol^{-1} than the alternative structure with a torsion angle of 76.2^o without a hydrogen bond. This result confirms that the lowest energy conformation of **1a**, shown in Figure 4, contains an intramolecular hydrogen bond,[39] a result consistent with the experimental crystal structures.[35-36, 40] These calculations were repeated using the PCM[41] continuum solvent method with a dielectric constant of 78.8, appropriate to water, and the difference in energy for the two conformations decreased to 2.6 kcal mol^{-1} which is smaller than the 4.5 kcal mol^{-1} difference calculated in the gas phase but still significant.

10.1002/chem.201605099

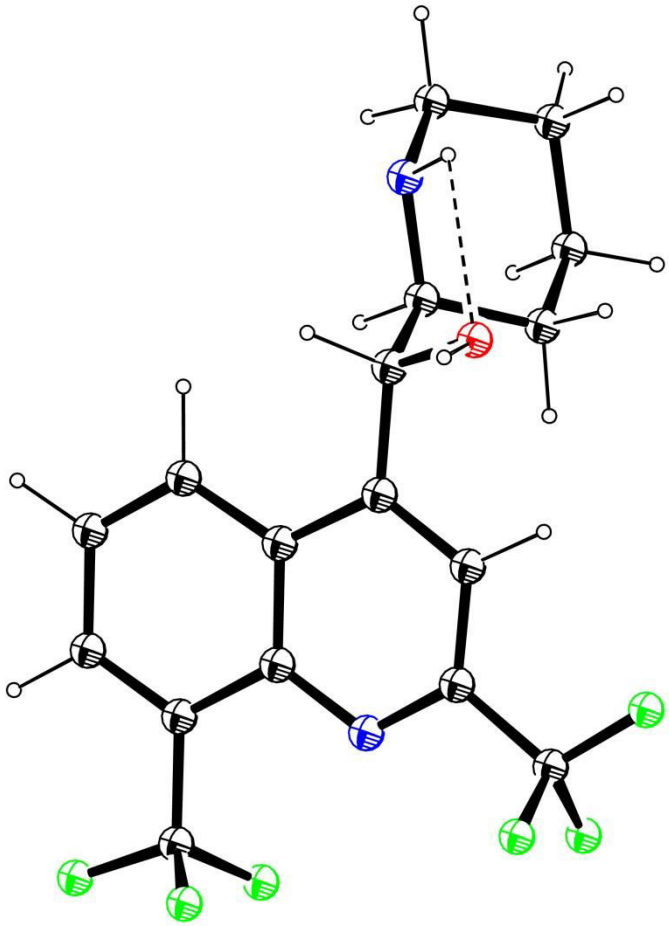

Figure 4. The lowest energy conformation of **1a**. Carbon black, nitrogen blue, oxygen red, fluorine green. The intramolecular hydrogen bond is shown as a dotted line.

The protonation preferences of **1a** were investigated because they may assist in defining electrostatic interactions with the putative heme receptor. The crystal structures of the protonated **1a** all show that the exocyclic nitrogen is protonated in preference to the aromatic nitrogen. This result was consistent with observed crystal structures for both quinine and quinidine salts. The energies of the protonated mefloquine ions showed a difference of 6.6 kcal mol^{-1} in favour of protonation at the exocyclic piperidine nitrogen. This result was consistent with crystallographic observations.[35-36]

10.1002/chem.201605099

This preference of side chain protonation was also consistent with the fact that similar molecules, such as quinine and quinidine, were also initially protonated on the aliphatic nitrogen rather than the aromatic nitrogen atom. The pKa values of quinine have been measured as 8.6 for the aliphatic and 3.5 for the quinoline nitrogen atoms,[42] respectively.

Establishing the effect of the substituent CF_3 groups that gave rise to this result was important. Accordingly, model compounds **1b** (mefloquine with the CF_3 group in position 2 removed and replaced by hydrogen), **1c** (mefloquine with the CF_3 group in position 8 replaced by hydrogen) and **1d** (mefloquine with both CF_3 groups replaced by hydrogen) were created. The structures of these compounds were optimized with protonation at either type of nitrogen. The resulting energies, given in Table 3, showed that the presence of the CF_3 group in position 2 significantly decreased the likelihood of the adjacent aromatic nitrogen being protonated in preference to the aliphatic nitrogen atom, whereas the presence of the CF_3 in position 8 had a much smaller effect.

Table 3. The energies in the gas phase calculated with DFT methodology with either the aliphatic (endocyclic piperidinyl) or aromatic nitrogen (endocyclic) atoms protonated. Also, included were values from models created from mefloquine by omitting specific CF_3 groups.

	Energies/kcalmol^{-1}
	aliphatic N protonated – aromatic N protonated
mefloquine **1a**	-6.6
1b	0.7
1c	-5.8
1d	2.1

10.1002/chem.201605099

The two CF_3 groups allow, in principle, the formation of an internal bifurcated hydrogen bond to the adjacent protonated aromatic nitrogen. If such an interaction was possible, this could occur either from the CF_3 group in the 2 or 8 position. From the CF_3 group in the 2-position, the fluorine would be in the plane of the quinoline-ring and the F...H distance would be 2.14 Å with an N-H...F angle of 104.6°. From the CF_3 group in the 8-position, a fluorine substituent in the plane of the aromatic ring would be 1.60 Å from this hydrogen with an N-H…F angle of 129.6°.

There were, however, no examples in the Cambridge Crystallographic database[43] of either hydrogen bond formation, an observation that suggested that it is not likely to occur. However, what is clear is that the introduction of CF_3 groups in either position 2- or 8- of the quinoline ring causes steric crowding around the aromatic nitrogen (whether protonated or not) that will modulate efficient interaction of this atom with the heme receptor.[23]

Calculations for **2** were repeated after geometry optimization showed an inter-ring angle of 9.9° between the phenyl ring in position 2 and the aromatic system. The energy for the conformation with a torsion angle for O-C-C-N of -67.5° containing a hydrogen bond was lower by 3.9 kcal mol^{-1} than that of the alternative structure with a torsion angle of 75.4°. When the calculations were repeated in a water environment, this second structure became the more favourable but only by 0.5 kcal mol^{-1}. The lowest energy conformation is shown in Figure 5.

10.1002/chem.201605099

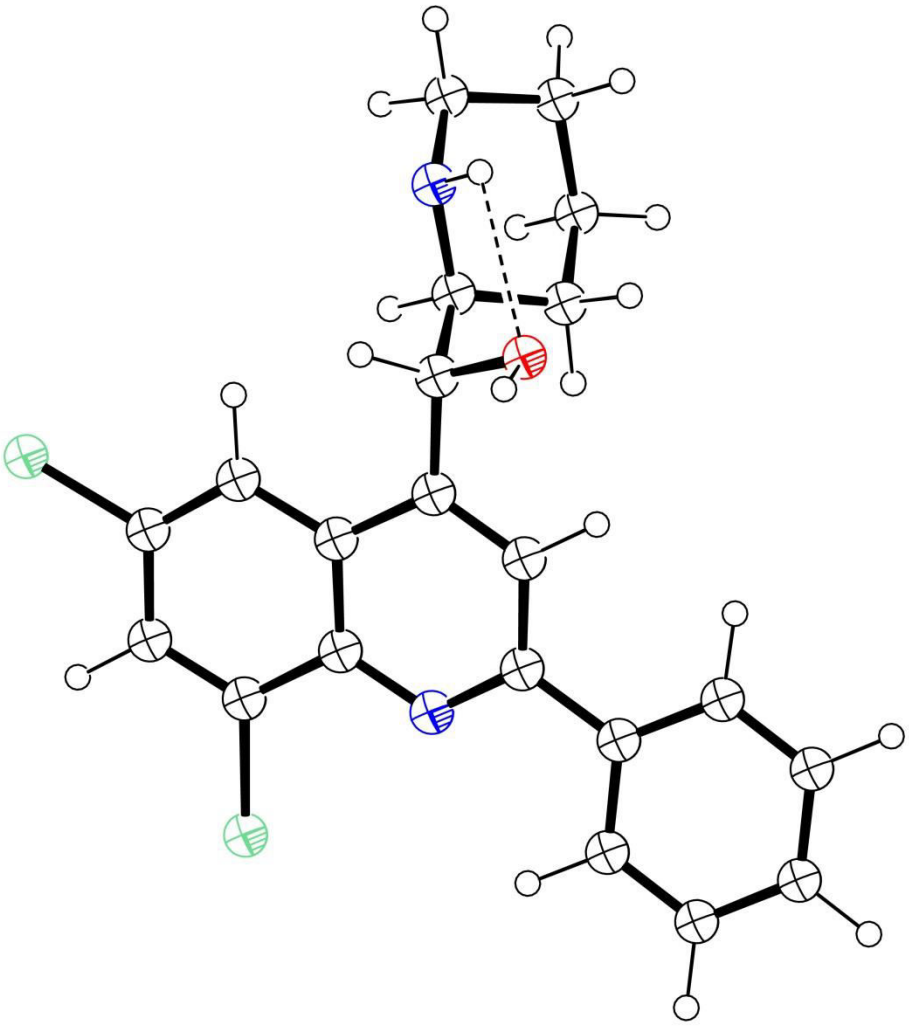

Figure 5. The lowest energy conformation of **2**. Carbon black, nitrogen blue, oxygen red, chlorine green. The intramolecular hydrogen bond is shown as a dotted line.

The energies of the protonated compounds were next calculated for the conformations with a hydrogen bond. These showed a preference for the aromatic nitrogen by 4.2 kcal mol^{-1} rather than the aliphatic nitrogen, thus the reverse situation to **1a**. The phenyl ring substituent in the 2-position clearly has the opposite effect to that of the CF_3 groups in **1a**.

A similar calculation was carried out for chloroquine **4a**, using the crystal structure of the diprotonated diphosphate monohydrate[44] as the starting model. There were three possible nitrogens to be protonated: the aromatic nitrogen, the exocyclic 4-amino nitrogen and the

diethyl aliphatic side chain nitrogen. The relative energies were calculated as 0, 34.1, 13.0 kcal mol^{-1} respectively, a result consistent with the crystallographic results but not with experimental data[45] that show that the monocation resides almost exclusively in the alkyl amino protonated form (pK_{a1} = 7.94 +/- 0.02; pK_{a2} = 10.03 +/- 0.02) whereby ionization of **4a** is controlled mainly by the change in enthalpy due to the significantly higher values of ΔH^o compared with the entropic component, $T\Delta S^o$.[45]

Subsequently, the structure of **5**, Ro 47-7737 was investigated. There are two chiral carbon atoms, the two carbon atoms in the cyclohexane ring that are bonded to nitrogen. These give rise to two different isomers *trans* (*R,R*) and *trans* (*S,S*) (Figure 6). The structural *cis*-isomer was also investigated.

The possible conformations of **5**-*trans* (*R,R*) and **5**-*cis* (*R,S*) structures were investigated with molecular dynamics and subsequent molecular mechanics energy minimization, which was followed by geometry minimization on the lowest energy conformations with the Gaussian09 program.[38] Utilizing molecular mechanics calculations, two low energy conformations were established for the (*R,R*) conformation with the two nitrogen atoms in equatorial positions (eq,eq) relative to the cyclohexane ring in the chair conformation but on DFT minimization, these two converged to an equivalent geometry. In addition, a third configuration named **5C** with the two nitrogen atoms in axial positions (ax,ax) was established.

The eq,eq conformation **5**-*trans* has the lowest energy with the ax,eq and ax,ax conformations having higher relative energies by 5.1, 7.0 kcal mol^{-1}, respectively. These relative energies increased significantly in water to 7.7, 8.6 kcal mol^{-1}. These results can be compared with an energy difference found by Karle *et al*[36] at the HF/6-311G level of 11.3 kcal mol^{-1}in favor of the (eq,eq) configuration over the (ax,ax) configuration for the

10.1002/chem.201605099

diprotonated compound.[2a, 36] The conformations can be characterized by the central torsion angles involving atoms C41-C32-N31-C1-C6-N11-C12-C21 (Figure 7).

These angles were respectively -1.1, 158.2, -53.3, 158.7, -1.2°: -11.1, 111.7, -55.2, -101.0, 135.5°; and -127.9, 87.1, -165.6, 79.4, 0.0° for the **5**-*trans* (eq,eq), **5**-*cis* (ax,eq), and **5C** (ax,ax) conformations respectively. The first conformation **5**-*trans* (eq,eq) was similar to that observed in the crystal structure of **7a** (see later, Figure 7). A slightly different eq,eq conformation was observed in the crystal structure of the diprotonated dimethylsulfonate salt [40] where the torsion angles were 8.9, 103.3, -62.0, 104.2 -11.0°. Although this conformation was established as distinct in molecular mechanics calculations, as stated above, it converged to the aforementioned eq,eq structure on energy minimization with DFT.

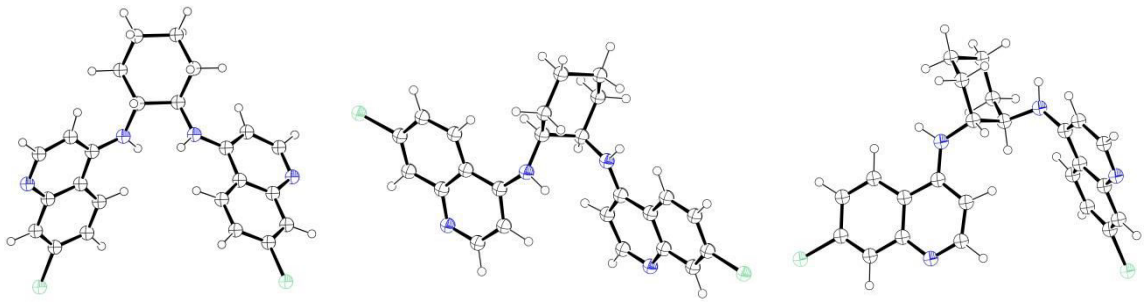

(a) (b) (c)

Figure 6. Lowest energy conformers of (a) **5**-*trans* (R-R) (eq-eq), (b) **5**-*cis* (*R*-*S*) (ax,eq) and **5C** (R-R) (ax,ax).

In order to investigate the protonation pattern of the ligand, the eq,eq conformation of **5**-*trans* was chosen because it had a) the lowest energy and b) the crystal structure of the related **7c**-*trans* has been determined. This ligand (**5**-*trans*) was first protonated via one of the aromatic nitrogen atoms and then on a 4-amino exocyclic nitrogen atom to give relative energies of 0.0, 32.0 kcal mol^{-1}, respectively, a result which is consistent with the observation

in chloroquine **4a** that the 4-amino nitrogen atom is an unlikely site for protonation. Similar differences in energies were obtained with the other two configurations **5**-*cis* and **5C**.

Then two equivalent nitrogen atoms were protonated, the resulting energies in the (eq,eq) configuration in the gas phase were lower by 107.7 kcal mol^{-1} for two aromatic compared to two 4-amino exocyclic nitrogen atoms, a value that was more than twice that for the monoprotonated compounds, presumably because of the close proximity of the protonated 4-amino exocyclic nitrogen atoms to each other. This observation was in agreement with the crystal structure of the (*R,R*) configuration, where the hydrogen atoms were located on the two aromatic nitrogen atoms in the diprotonated compound[40] and, indeed, form donor hydrogen bonds to the anions. These observations are consistent with a published biophore in which the endocyclic nitrogens act as proton acceptors while the secondary 4-aminoquinoline groups act as donors.[2, 23]

Structures of **6**-*trans* and **7c**-*trans* were also studied by constructing starting models from the lowest energy (eq,eq) conformation of the *trans* **5**-*trans* (*R,R*) configuration obtained previously. CF_3 groups were subsequently added into position 7 for **6**-*trans* and both 2 and 8 for **7c**-*trans* and results are compared to those for **5**-*trans* in Table 5.

Table 5. Comparison of energies (kcal mol^{-1}) for structures **5**-*trans*, **6**-*trans*, **7a**-*trans* and **7c**-*trans*.

	ΔE_1 [i]	ΔE_2 [ii]
5-*trans*	256.0	32.0
6-*trans*	263.1	31.8
7a-*trans*	253.0	33.8
7c-*trans*	244.3	34.7

[i] ΔE_1 = E(compound) – E(compound)H^+, protonated at the aromatic nitrogen.

[ii] ΔE_2 = relative energy of compound protonated at the exocyclic nitrogen compared to the aromatic nitrogen.

10.1002/chem.201605099

The results shown in Table 5 allowed several conclusions to be drawn. First, the protonation preferences for the bisquinolines **5**-*trans*, **6**-*trans*, **7a**-*trans* and **7c**-*trans* were the opposite of those observed in **1a** with the bisquinolines favoring aromatic protonation and with mefloquine **1a**, aliphatic protonation in the gas phase, although it should be noted that the differences in energy for the bisquinolines were much larger than that for **1a**. Indeed, protonation at the exocyclic nitrogen was very unfavorable for all four structures, the energy differences for all three molecules being over 31.7 kcal mol^{-1}. Comparison of the protonation energies showed that the replacement of Cl with CF_3 in the 7 position or the inclusion of CF_3 groups in the 2 and 8 positions induced only a small effect upon the preferences. The crystal structure of **7c**-*trans* (R-R) was determined by X-ray crystallography and is illustrated in Figure 7.

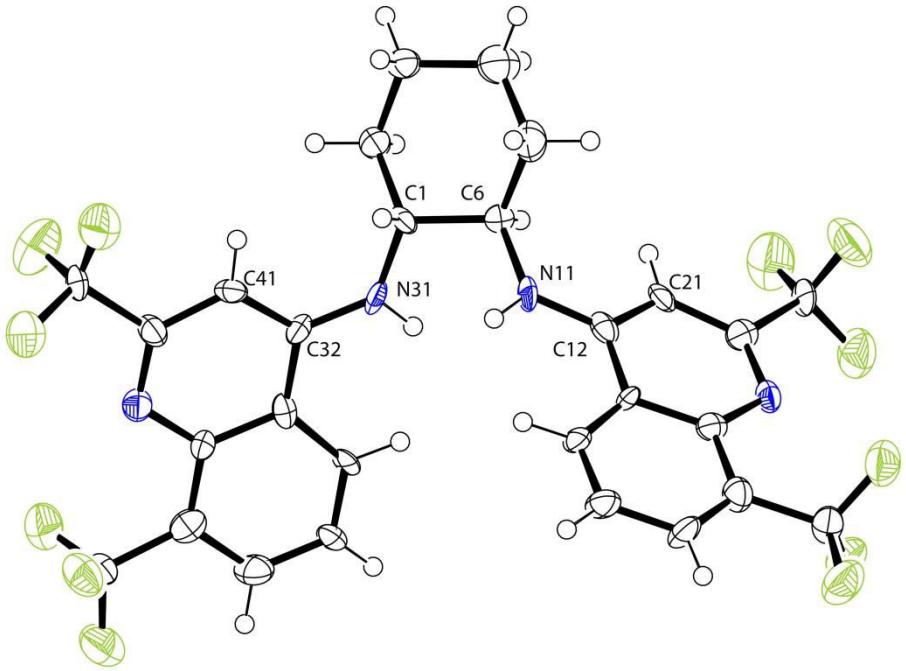

Figure 7. The structure of **7c**-*trans* as determined by X-ray crystallography with ellipsoids at 50 % probability. The solvent methanol molecule is not shown.

10.1002/chem.201605099

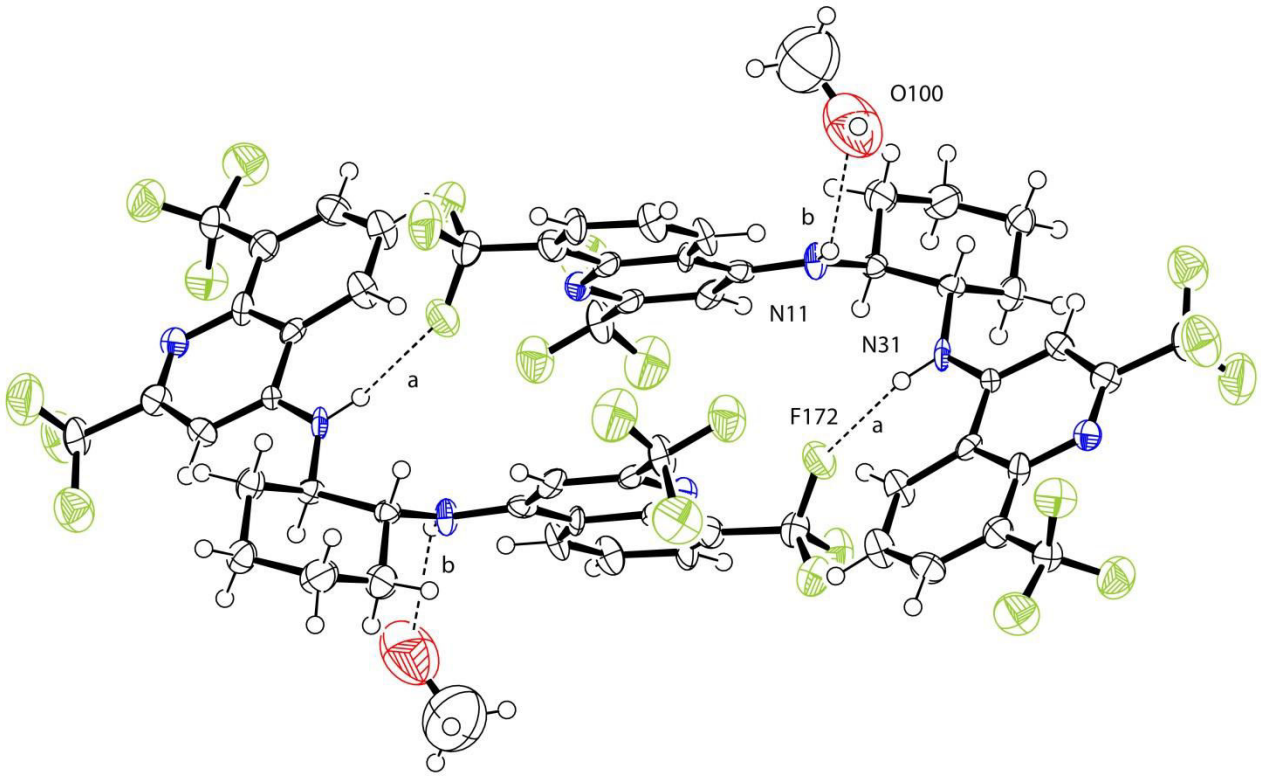

Figure 8. The structure of **7c**-*trans* showing the formation of a centrosymmetric dimer facilitated by N31-H…F172 hydrogen bonds labelled as a. The N(11)-H atom formed a hydrogen bond, labelled as b, to the oxygen atom O(100) of a methanol solvent molecule. Hydrogen bonds a and b are shown as dotted lines.

The five torsion angles in the C41-C32-N31-C1-C6-N11-C12-C21 link were 1.7, 164.0, -52.2, 154.6, -5.5° so the conformation was very similar to that obtained from the conformational analysis of **5**-*trans* described above where the angles obtained were -1.1, 158.2, -53.3, 158.7, -1.2°. The minimal difference indicates that the crystal packing, which involves the formation of a centrosymmetric dimer in which the two molecules are connected by hydrogen bonding between N31 and F172 (symmetry operation 1-x,1-y,-z) at 3.30 Å with H…F 2.53 Å and N-H…F 149° as shown in Figure 8, has little effect on the conformation. From Figure 8, it is apparent that the two aromatic rings at the centre of the

dimer are perforce parallel but the distance between them is ca 4.0 Å which is too long to indicate a significant π…π interaction. The angle between the two 10-membered aromatic moieties in the two halves of the molecule is 64.7°, thus the molecule is far from planar which has significant implications for its interaction with heme as discussed later. In addition, N11 forms a hydrogen bond to a methanol solvent molecule (N11-H…O100 N…O 2.93, H…O 2.22Å, N-H…O angle 141°), as also seen in the COSY spectrum (Figure 3). Notably, the solvent methanol forms close contacts to F374, F404, F372 (symmetry operation -x,-y,-z-1) with O…F distances at 2.97, 3.15, 3.33 Å shown in Figure S34. The significance of the formation of all these hydrogen bonds is clearly a crucial factor in the chemistry of **7c**-*trans* and is further explored when considering the interactions of molecules, **5**-*trans*, **6**-*trans*, **7c**-*trans* with heme (see later).

Binding of ligands to heme

Antimalarial drug design was historically hampered by assuming a drug target whose identify shifted according to the popularity of known research from heme to DNA to proteins and other targets.[46] Consequently, initial work by Ismail[2a, 22] employed an extra-thermodynamic approach to 4-aminoquinoline and 4-aminobisquinoline drug design, in which details of molecular interactions were not required.[47] Initially, speculation that a protein receptor could also be a drug target[48] then led to determination of putative maximum volumes of the receptor site (assuming it could be a macromolecule). This type of approach is now re-gaining favour and recognition of some of the limitations of target-based drug discovery,[49] has prompted a "renaissance of a more holistic approach in which complex biological systems are investigated for phenotypic changes upon exposure to small molecules." [50] Currently, in line with most investigators, the currently favoured 4-aminoquinoline drug target is heme, released during the catabolism of hemoglobin. Although,

various proteins are now known to be also involved in processing heme within the parasite, including recently identified heme detoxification proteins[2a, 4a, 51] and kinases,[49a] it is currently unknown if 4-aminobisquinolines target such processes. Consequently, investigations interrogating the nature of various bonding interactions were considered using computational approaches and were limited only to heme.

Dascombe *et al*.,[23] postulated that metaquine (**10**, Figure 1) could be complexed to hematin in several modes, especially via several non-bonded contacts including two intramolecular hydrogen bonds, one from an exocyclic N-H in **10** to the axial hydroxyl group in hematin and the second from the associated endocyclic quinoline nitrogen atom to the carboxyl group in hematin. This was dubbed an "above face" interaction (i.e. that containing the axial hydroxyl group) as opposed to binding on the obverse (below) face, which favors π-π interactions with suitable drugs. A previous modeling study[52] on chloroquine **4a** concentrated on this obverse binding and found significant π-π interactions but above face interactions were not considered. It will be noted that compounds **5**, **6** and **7c** (Figure 1) all contain a cyclohexane bridge between two aromatic moieties, which creates a very different shape and therefore interactions with the receptor were likely to be different from those involving **10** and for that matter **4a**.[23] One major change was that in the *trans* isomers of **5**-*trans*, **6**-*trans*, **7c**-*trans*, it might be possible for both exocyclic N-H groups to hydrogen bond to the hydroxyl group. In addition, the existence of the CF_3 groups in **6** and **7** permit alternative hydrogen bonding from the carboxylic acid group to a fluorine rather than to the endocyclic nitrogen atom. Indeed it could also be possible for the chlorine in **5** to be involved in such an interaction.

These possibilities were first investigated by molecular mechanics using the Cerius2 software[51] with the Universal Force Field and the most likely resulting structures were optimized. Calculations on these structures were then carried out using density functional

theory methods as implemented in Gaussian-09,[38] following methods and procedures as reported and tested previously.[53] In general, the unrestricted B3LYP hybrid density functional theory was used for all geometry optimizations and frequencies.[54] All structures were optimized with an LANL2DZ basis set on iron (with core potential) and 6-31G* on the rest of the atoms (H, C, N, O): basis set BS1.[55] It was assumed in all calculations that iron was Fe(III) with five unpaired electrons so molecules were neutral when a hydroxide was present and +1 otherwise.

In the starting models, the ligands were given their lowest energy conformations and hematin its crystal structure.[56] Models of **5**-*trans*, **6**-*trans* and **7c**-*trans* were complexed with heme in several different ways based on our current knowledge of the system. The crystal structure of both heme[56a] and a limited number of antimalarials of the quinoline methanol class covalently bound to heme have been obtained but the 4-aminoquinoline class has proved elusive[56b] and investigators have resorted to EXFAS studies and modelling studies.[21] Consequently, it has been shown that the mode of action of quinoline methanols is at heme but unlike 4-aminoquinolines, they displace the axial group to form a Fe-O bond which is also found in all other compounds of this class (e.g. halofantrine,[57] Cinchona alkaloids especially **3**[58] and **1a**).[59] This type of covalent adduct can enforce a π-π interaction between ligand and receptor to minimize intramolecular interactions.

In terms of frequency, the most popular literature depiction is a π-π type interaction between ligand and heme receptor,[60] followed by some studies invoking a metal-N bond.[61] In contrast, models invoking electrostatic interactions (hydrogen bonding) have occasionally[62] been investigated and indeed such an arrangement has subsequently been found in a crystal structure of a gallium hemozoin analogue-chloroquine complex (but not with the monomeric heme considered in the current study).[63] Studies have also considered

interactions with a heme μ-oxo dimer using EXAFS[21, 64] but these were beyond the scope of the current investigation.

Following these precedents, several modes of interaction of molecules **5**-*trans*, **6**-*trans*, **7c**-*trans* with heme were considered. These included structures of various types: (a) in which the ligand displaced the hydroxide and an Fe-N bond was formed (complexes 1 and 2, Figure 9); (b) in which the ligand was positioned to the edge of the heme forming hydrogen bonds to the carboxylic acid groups of the heme (complexes 3 and 4, Figure 10); (c) structures with the ligand on the obverse face (complexes 5-8, Figure 11 and 12); (d) structures with the ligand forming above face contacts (complexes 9-12, Figure 13) and (e) structures were created in which two ligands were involved on either side of the heme (complexes 13, 14, Figure 14). Finally, a calculation was carried out for a heme-mefloquine complex (complex 15, Figure 15).

The structures minimized by molecular mechanics were then reinvestigated by DFT calculations as previously described. The energies of interaction were calculated as E(complex) – E(Heme) – E(ligand) with E(OH) also included when present.

The structures obtained all converged satisfactorily and are illustrated in Figures 9-15. Details of the calculations and coordinates are included in the Supporting Information.

10.1002/chem.201605099

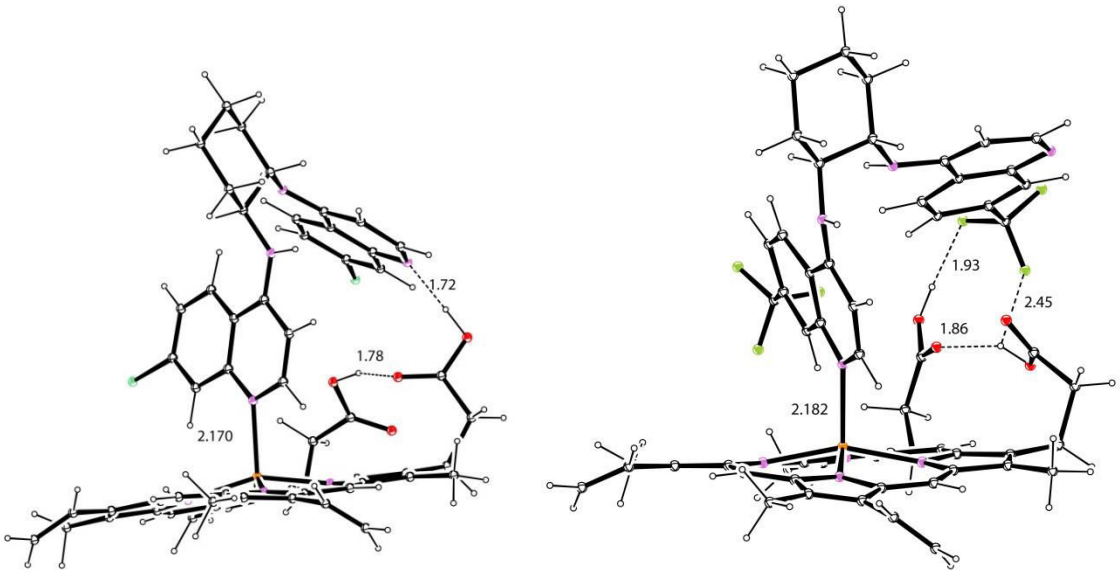

Figure 9. DFT optimized structures of complexes 1 and 2, with distances in Å. Hydrogen bonds shown as dotted lines.

Structures of complexes 1 and 2 containing ligands **5**-*trans* and **6**-*trans*, respectively, are shown in Figure 9 and are particularly interesting as the input models included a Fe-N(quinoline) bond but no additional hydrogen bond. However, on geometry optimization of complex 1, two hydrogen bonds were formed, one between an OH from a porphyrin propionic acid group and a quinoline nitrogen atom with O-H…N 1.72 Å and the other between carboxylic acid groups with O-H…O 1.78 Å respectively both distances indicating strong hydrogen bonds. The energy of interaction was calculated as -36.7 kcal mol^{-1}.

The structure of complex **2** also contained donor hydrogen bonds from the carboxylic OH groups but in this case the O-H that formed a hydrogen bond to the second carboxylic OH group with O-H…O 1.90 Å also formed a weak hydrogen bond to a fluorine atom O-H…F 2.45 Å. This second carboxylic OH group formed a strong hydrogen bond to a second fluorine atom O-H…F 1.93 Å, thus very different to that observed in complex 1, in which this oxygen forms a hydrogen bond to nitrogen The difference between the two structures confirms our hypothesis expressed above that the CF_3 groups in **6** and **7** could readily be used

to stabilize the complex. The energy of interaction was similar to that in found for complex 1 at -35.5 kcal mol^{-1}.

The structures of complexes 3 and 4 containing ligands **5**-*trans* and **6**-*trans* respectively with edge type interactions followed similar patterns to orientations established in our previous work[23, 62] for other ligands in that the ligands were positioned forming hydrogen bonds to the two carboxylic –OH groups. The structures were very similar in which the two quinoline nitrogen atoms act as acceptors with O-H…N distances of 1.72 and 1.80 Å in complex 3 and 1.73, 1.81 Å in complex 4. The energies of interaction at -16.7, -24.4 kcal mol^{-1} respectively were significantly less than that observed for complexes 1 and 2. This is opposite to the relative interaction energies found where the energy of the edge type interactions was favoured in both chloroquine **4a** and metaquine **10** (data not shown)[65] over the covalent bond structure presumably because of the interactions imposed by the folded nature of ligands **5**-*trans* and **6**-*trans*.

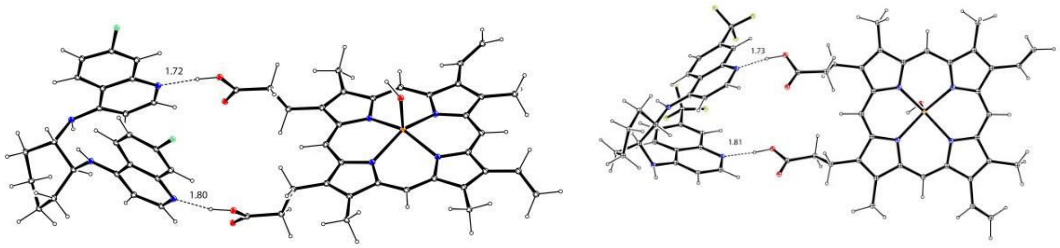

Figure 10. DFT optimized structures of complexes 3 and 4 showing edge-type interactions with distances in Å. Hydrogen bonds shown as dotted lines

The structures of complexes 5 and 6, shown in Figure 11 with ligands **6**-*trans* and **7c**-*trans*, respectively, are particularly interesting in that they converged to structures very different from the input structures which contained π…π stacking between the heme and the

10.1002/chem.201605099

ligand on the obverse face in a planar conformation. The conformation of the ligand totally changed to a folded geometry closer to the energy minimum discussed above.

In the structure of complex 5, four close interactions were observed, the shortest being one between a methyl hydrogen from the heme to a fluorine H…F 2.44 Å. There were also two interactions between C-H groups from the ligand and two of the nitrogen atoms in the heme (H…N 2.73, 2.89 Å). There was also an O-H…N interaction with H…N 1.875 Å .However the energy of interaction for this structure was only -8.8 kcal mol^{-1}.

In the structure of complex 6, there is a hydrogen bond between the carboxylic acid oxygens O-H…O 1.95 Å while the other significant interactions are between a methyl hydrogen on the heme which forms close contacts to two fluorine atoms from different CF_3 groups at 2.79, 2.64 Å. In addition a hydrogen atom from a $=CH_2$ group forms a contact of 2.55 Å with a fluorine atom. Thus, both CF_3 groups in **7c**-*trans* form contacts with the heme, but the resulting energy of interaction is a small -4.9 $kcalmol^{-1}$.

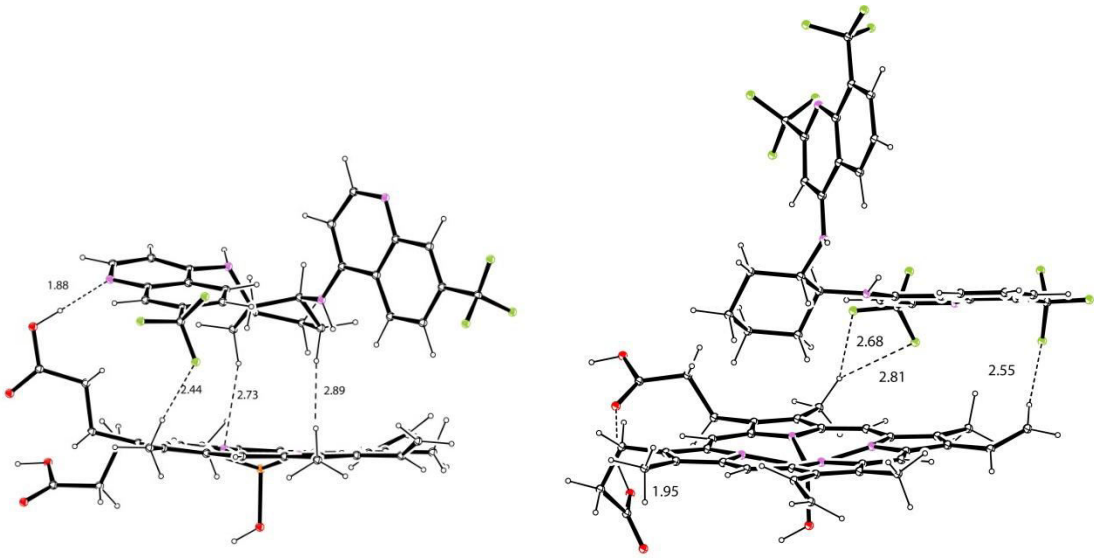

Figure 11. DFT optimized structures of complexes 5 and 6 with distances in Å. Hydrogen bonds shown as dotted lines

10.1002/chem.201605099

The structure of complex 7, shown in Figure 12 was created in an attempt to ascertain whether one or both carboxylic acids could enter into the cavity between the two aromatic sections of **7c**-*trans*. The input model contained both carboxylic acids in the cavity, but the final optimized structure contained only one which formed a donor hydrogen bond to a fluorine atom (O-H…F 1.98 Å). In addition there was a hydrogen bond between carboxylate oxygens atoms with (O-H…O) 1.90 Å. The energy of interaction is -11.7 kcal mol^{-1}.

The structure of complex 8, shown in Figure 12, involved an attempt to stack the two molecules involving π…π interactions. The ligand was placed on the opposite side to the hydroxide on heme (e.g. the obverse face). In the resulting structure the main interactions are between a carboxylic acid and the ligand, via O-H…F interaction of 2.01 Å and a C-H…O interaction from the ligand to the second oxygen of 2.36 Å. In addition there are weak interactions from a methyl hydrogen to F at 2.54 Å and an aromatic C-H to N(heme) at 2.58 Å as shown in Figure 12. The energy of interaction is -9.6 kcal mol^{-1}

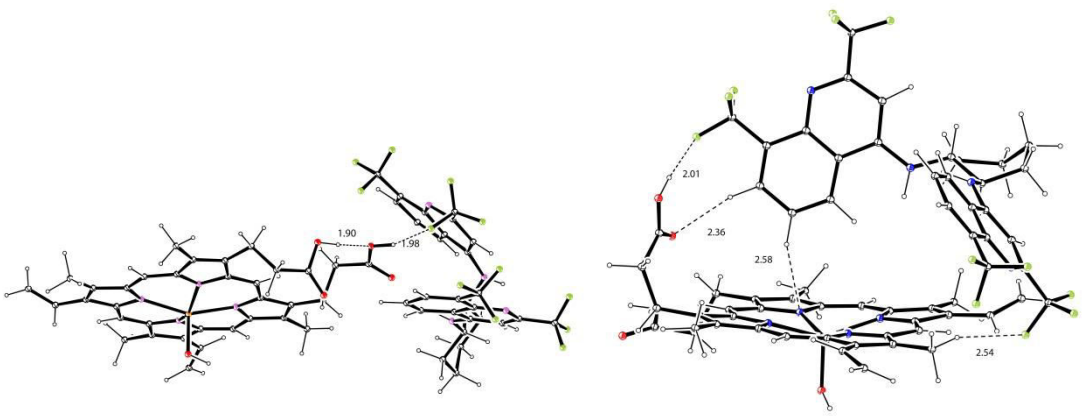

Figure 12. DFT optimized structures of complex 7 and 8 with distances in Å. Hydrogen bonds shown as dotted lines

10.1002/chem.201605099

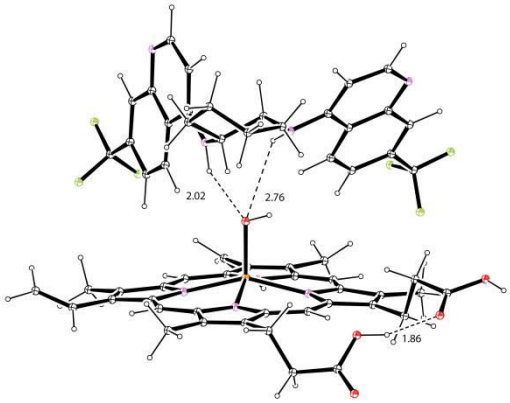

Complex 9

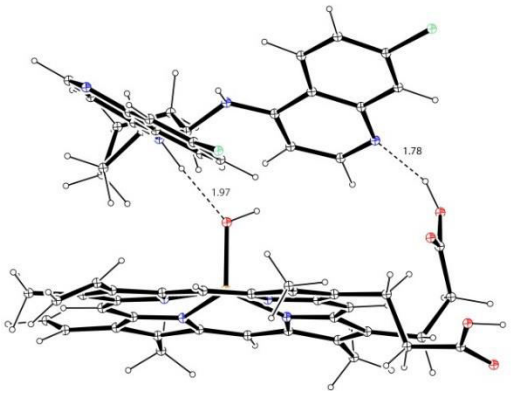

Complex 10

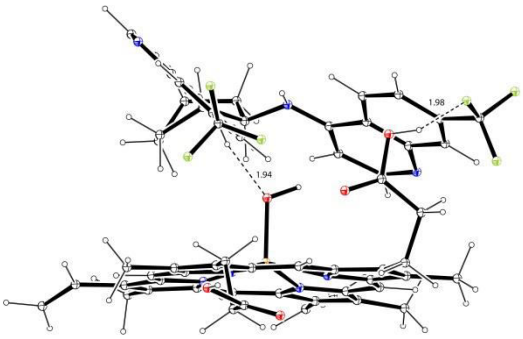

Complex 11

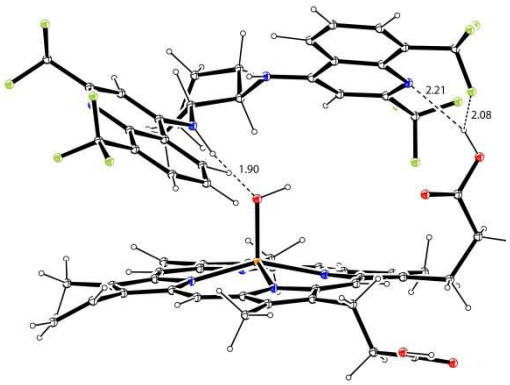

Complex 12

Figure 13. DFT optimized structures of complexes 9, 10, 11 and 12 with distances in Å. Hydrogen bonds shown as dotted lines

The structure of complex 9 which contains **6**-*trans*, shown in Figure 13 was an attempt to ascertain if a stable structure could be obtained in which the two exocylic N-H bonds could both form hydrogen bonds to the heme hydroxide. In the event, the two N-H…O distances optimized to 2.08, 2.78 Å so there are significant interactions but with one much shorter than the other. Presumably the presence of the hydrogen on the oxygen atom in the hydroxide precludes both N-H groups from forming similar short interactions. This structure

also contains an intramolecular hydrogen bond between carboxylic acid groups with O-H…O 1.92 Å. The energy of interaction was quite favorable at -20.0 kcal mol^{-1}

Three further complexes 10, 11 and 12 involving **5**-*trans*, **6**-*trans* and **7c**-*trans* respectively were also built to investigate the interaction of the two exocyclic N-H bonds with the heme hydroxide. In these cases the starting model including two hydrogen bonds from N-H to O but in the optimized structures, shown in Figure 13, only one such interaction was maintained with the other H…O distance increasing to > 4.0 Å. However, in addition to one N-H…O hydrogen bond at distances 1.97, 1.94, 1.90 Å, the optimized structures showed different additional hydrogen bonds involving a carboxylic OH group. In complex 10, containing **5**-*trans*, there is an O-H…N hydrogen bond at 1.78 Å, in complex 11 containing **6**-*trans*, a O-H…F hydrogen bond at 1.99 Å while in complex 12 containing **7c**-*trans* the O-H forms a bifurcated hydrogen bond to F at 2.08 Å and N at 2.21 Å. Despite these differences the energies of interaction for the three complexes were very similar at -19.0, -18.3, -19.0 kcal mol^{-1}, respectively.

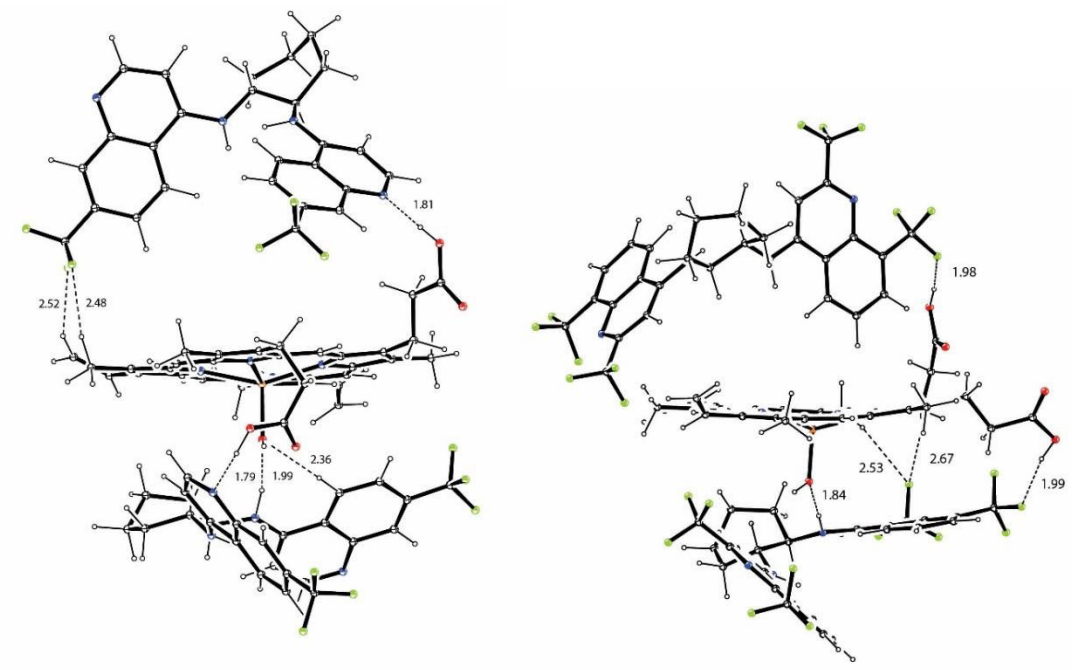

Figure 14 DFT optimized structures of complexes 13 and 14 with distances in Å. Hydrogen bonds shown as dotted lines

10.1002/chem.201605099

The structures of complexes 13 and 14 which involve two ligands (6-*trans*, 7c-*trans* respectively) sandwiching one molecule of heme are shown in Figure 14. As might be expected, the two structures show both obverse and above face interactions, which have been observed previously in the models with just one ligand. For example complex 13 exhibits three acceptor hydrogen bonds on the obverse face, namely an N…OH interaction with heme of 1.81 Å and two F…H-C interactions of 2.52 and 2.48 Å. On the above face, the ligand is involved in two donor hydrogen bonds, two to the heme hydroxide N-H…O of 1.99 Å and a C-H…O of 2.36 Å and an acceptor hydrogen bond from a carboxylic acid oxygen N…H-O at 1.79 Å.

A different pattern of bonding is observed from complex 14 where there is only one significant obverse face interaction of O-H…F 1.98 Å, but several above face including strong N-H…O 1.84, O-H…F 1.99 Å and weak hydrogen bonds C-H…F of 2.53 and 2.67 Å. It is thus apparent that in both structures the interactions are stronger on the above face side. It is also noteworthy that in both structures, the two carboxylic acids are hydrogen bonded to the ligands on opposite sides. The interaction energies are -42.2, -21.3 $kcalmol^{-1}$ respectively showing that the interactions are far stronger in 13 than in 14.

The final structure in this section shows a possible structure for protonated mefloquine forming complex 15 with heme, shown in Figure 15.

10.1002/chem.201605099

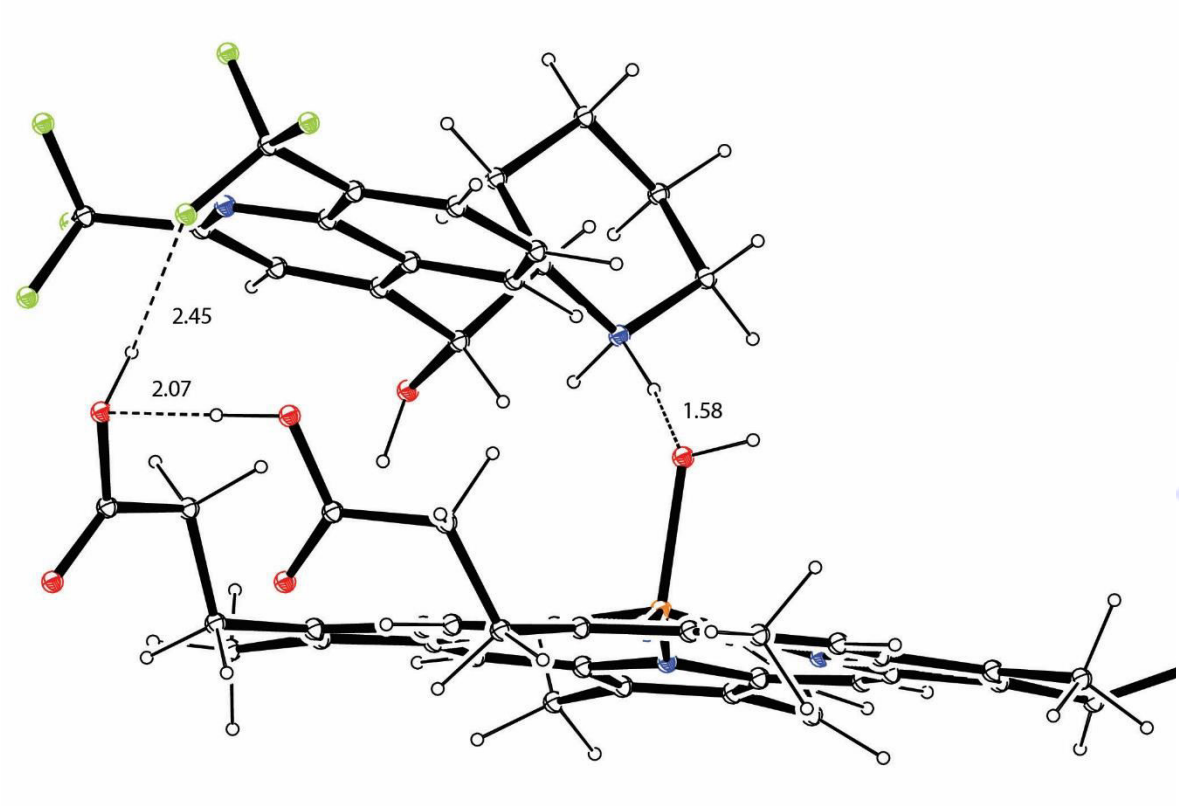

Figure 15. DFT optimized structures of complex 15 showing edge-type interactions with distances in Å. Hydrogen bonds shown as dotted lines.

In this structure the mefloquine was protonated at the aliphatic (piperidyl) rather than the aromatic nitrogen, consistent with the calculations above and crystallographic observations. This hydrogen atom formed a very strong hydrogen bond to the heme hydroxide with N-H…O 1.58 Å. Other hydrogen bonds involved two carboxylic oxygen atoms O-H…O 2.07 and an O-H…F between the ligand and heme of 2.45 Å. The energy of interaction was -40.2 kcalmol^{-1}. Therefore, it could be considered to pre-organize this fluorinated quinolone methanol to attack heme by forming an axial Fe-O(alkoxide) bond as seen in crystal structures.[59] But, an equivalent 4-amino-quinoline crystal structure, such as for chloroquine **4a**, has yet to be found.[61]

Table 6. Interactions energies (kcal mol^{-1}) for complexes 1-15 in the gas phase and in water.

Complex	ΔE(gas)	ΔE(water)
1	-36.7	-24.3
2	-35.5	-23.4
3	-16.7	-14.0
4	-24.4	-20.7
5	-8.8	-6.9
6	-4.9	-4.3
7	-11.7	-5.0
8	-9.6	23.0
9	-20.0	-10.0
10	-19.0	-10.4
11	-18.3	-11.2
12	-19.0	-8.7
13	-42.2	-33.9
14	-21.3	-9.6
15	-40.2	-15.4

Of course the interaction of ligands with heme does not occur in the gas phase and therefore the calculations were repeated in the solvent water PCM method in Gaussian09.[38] The same starting models were used as in the gas phase calculations, but notably the structures refined to similar structures. The energies of interaction are compared to those from the gas phase in Table 6. While the order of ΔE values remains the same, with complexes 1 and 2 which contain a Fe-N bond having the prefered values of -24.3, -23.4 kcal mol^{-1}, complexes 3 and 4 with edge-type interactions now give closer ΔE values at -14.0, -20.7 kcal mol^{-1}.

Several conclusions can be drawn from these DFT calculations. One general conclusion is the overriding importance of hydrogen bonds in the structures of these complexes. It is clear that in all structures, the relative positions of the heme and ligand are governed by the formation of hydrogen bonds. In all cases the carboxylic acid groups of the heme form hydrogen bonds, sometimes between each other but also with the exocyclic nitrogen, the quinoline nitrogen and/or the fluorine atoms of the CF_3 groups in **6**-*trans* and **7c**-*trans* although no hydrogen bonds were found with the chlorine atoms in **5**-*trans*. While not in itself viable having a relative small interaction energy, the structure of complex 6 is

particularly interesting as the ligand is linked to the heme via C-H…F rather than O-H…F hydrogen bonds. Taking the energies into account it can be concluded that the most likely structures are those which contain a covalent Fe-N bond (complexes 1,2) or the edge type interactions, (complexes 3,4), which are the most stable whether there is an hydroxide bonded to the iron or not. However, in the presence of the hydroxide, structures in which the ligand N-H moieties form hydrogen bonds to the hydroxide are also possible, although it would appear from the structure of complex 8 that one strong hydrogen bond could be formed. In all our studies we were unable to find a satisfactory low energy structure containing π…π stacking. Indeed it was found that any input structure containing stacking reverted on optimization to one containing hydrogen bonds involving one of the carboxylic acid groups of heme. The calculations on the sandwich complexes, 13 and 14 show that it is possible and indeed energetically favourable for two ligands to be attached to one heme but it is clear that the interactions on the above face are considerably more significant than those on the obverse face.

EPR Studies of Ligand-Heme Interactions

To investigate the interaction of one or more quinolines with the porphyrin, continuous-wave (CW) electron paramagnetic resonance (EPR) spectra (Figure 15) were recorded in order to investigate the spin state of the heme iron. The spectrum of hemin[ii] is typical of high spin ferric heme (S = 5/2) with turning points at $g_{\perp}^{eff}$ = 6.0 and $g_{\parallel}^{eff}$ = 1.99. On addition of 4-fold molar excess of either **5**-*trans*, **6**-*trans* or **7a**-*trans* under anaerobic conditions there was a dramatic ~65-95 % ±10 decrease in intensity of the ferric resonance without subsequent new signals. These observations suggest a change of iron spin state to an EPR silent species, possibly ferrous. This result clearly demonstrates for the first time that

[ii] Hemin chloride (hemin) is Fe(III)PPIX with a chloride ligand replacing the OH moiety.

binding allows a change of redox state in the porphyrin (Figure 14). The change of redox state of the heme was most pronounced for **5**-*trans* followed by **6**-*trans*, which was consistent with the relative antimalarial activity seen *in vivo*, on substituting the Cl with a CF_3 group against *Plasmodia*. Further work is needed in the future to unambiguously determine the spin states, as well as the electron source.

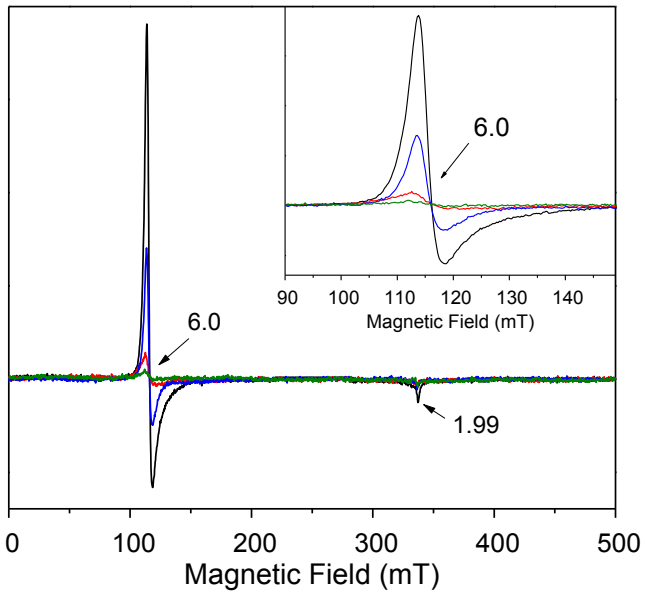

Figure 14. 9 GHz CW EPR spectra of a solution of 200 μM hemin (black), hemin on manual 5 sec mixing of 4-fold molar excess of **5**-*trans* (green), **6**-*trans* (red) and **7c**-*trans* (blue). Hemin concentration was 200 μM in all experiments. Inset shows magnification of the $g_{\perp}^{eff}$ region. Spectra were recorded at 5 K, 100 kHz, 0.4 mT modulation amplitude, 1 mW, 1 scan.

Implications for effective drug design

The results concerning the introduction of CF_3 groups into positions 2 and 8 in **7c**-*trans* agreed with previously reported structure-activity correlations.[3, 7-8, 10-11, 23, 25c, 27-28, 66] Introduction of a CF_3 group in position 7 proved to be superior in terms of antimalarial

activity over 2,7-di-trifluoromethyl substitution, which in turn is more active than 2,8-*bis*-trifluromethylated-*mono*-4-aminoquinolines analogs.

The interaction of the 2,8-trifluoromethyl bisquinoline with hematin falls into an anticipated order of stability from single crystal diffraction studies with hydrogen bonding[63] and covalent interactions dominating.[56b, 57-59] This evidence contradicts currently accepted models of drug antimalarial drug receptor interaction(s) since if the interactions between receptor and ligand were based on frequency of appearance in graphical forms then π-π depictions[22-23, 34n, 67] are most common and axial, covalent, coordinationed adducts[52, 56b, 57-61] are fewer in number. Edge type interactions between drug and ligand are currently restricted to a few studies only.[62-63] Hence, π-π interactions are often assumed to be preferred orientation geometry[68] between drug and porphyrin but to our knowledge, only one study compares the thermodynamics of a range of all three competing geometries,[62] which are essential for understanding antimalarial drug action.

As indicated for quinoline methanols for covalent binding,[59] the complex, in which the drug coordinates via an axial Fe-O(alkoxide) bond, appears to be the most stable, but having measured the Raman spectra for 4-aminoquinolines such as metaquine **10**[52] we previously failed to find convincing evidence of a Fe-N bond in solution as shown in Figure 9. Consequently, the two forms favored by thermodynamic considerations, both covalent and edge type hydrogen bonding interactions, require re-investigations where their importance to antimalarial drug interactions with the receptor can be further clarified by a suitable spectrometric study taking into account the various forms of hematin and hemin suggested to account for antimalarial drug action.[3b, 3c, 5, 20-21, 23, 29, 56, 60-61, 63-65]

For *bis*-trifluoromethylquinolines, the π-π type interaction was less stable than the corresponding hydrogen bonded mode which favours interaction at the secondary amine rather than the sterically encumbered nitrogen buttressed between the trifluoromethyl groups

(See Figures 7 and S15). This is consistent with sites of hydrogen bonding interactions seen both in solution by NMR (Figure 3) and in the solid state using crystallography.[23]

Conclusion

In conclusion, these results show that the inclusion of CF_3 substituents has a major impact on the geometry of drug interaction with the antimalarial heme receptor. This may explain why the substituent pattern present in **1a** is optimized for antimalarial activity only in the quinoline methanol class and this induces axial attack onto the porphyrin as verified recently by crystal structures.[59] Not only do the substituents affect the electronic properties of the molecule, they also offer alternative, preferential hydrogen bonding sites, and their steric bulk will reduce the possibility of interactions from the adjacent endocyclic nitrogen atom. Finally, both changes in redox state and geometry of binding to heme, when fully understood, could lead to the design of outstanding antimalarial drugs *in vitro* and *in vivo*.

Experimental

Solvents used in the reactions were purified according to standard methods. [63] All starting materials were of the highest purity available and were obtained from either the Aldrich Chemical Co., Lancaster Synthesis or Fluka. Chloroquine diphosphate was purchased from Sigma. Microanalyses were performed by MEDAC LTD, Brunel Science Centre, Egham, Surrey, UK and The Chemistry Department, University of Liverpool. Synthetic experiments were conducted using oven-dried glassware on a double vacuum manifold glass line under a protective atmosphere of dry argon.

All materials, whether synthesized in this laboratory, or purchased, were continuously purified until they demonstrated a single peak by GC-NMR and NMR spectroscopy (^{19}F and ^{1}H) to ensure that spectroscopic, physiochemical and pharmacological results were valid.

Melting points were determined using a Gallenkamp melting point apparatus and remain uncorrected but were verified by DSC.

Thin Layer Chromatography (TLC) was carried out on silica gel 60 glass backed plates using chloroform as eluant. Visualization was carried out either at 254 nm under UV light or in an iodine tank. Medium pressure chromatography was carried out using a custom made, one piece, all glass apparatus, foil covered packed with silica or neutral alumina (argon 1-15 bar). See Supporting Information for further details and spectra.

Spectroscopy

NMR spectra were recorded on Bruker AC-250, Avance 300 (5 mm BBO probe head) and Bruker Ascend 600 MHz Ultrashield nuclear magnetic resonance spectrometers. Spectrometer frequencies (and internal standards) were: ^{1}H: 250 MHz (TMS); ^{13}C: 62.896 MHz ^{19}F: 235.36 MHz ($CFC1_3$) or ^{1}H: 300.13 MHz (TMS); ^{13}C: 75.468. Peak multiplicity and partial connectivity was deduced using a combination of DEPT, APT, HMQC and ^{1}H-NMR experiments. DEPTQ experiment (16, 384 scans) was used to identify quaternary centers (see Supporting Information). Continuous-wave EPR spectra were recorded at 9.4 GHz on a Bruker EMX spectrometer with a Super-high-Q rectangular cavity and an Oxford ESR-900 liquid helium cryostat. The operating conditions are stated on the Figure legends.

Mass spectrometry experiments were performed using a VG MICROMASS 7070H, operated at 70 eV electron energy [Source temperature 200-250 °C; Scan time 3 seconds/decade from 750-720 Daltons (mass units)]. For chemical ionization (CI) experiments, the instrument was operated at 50 eV, and ammonia was used as the ionizing reagent. FT-IR spectroscopy was carried out using KBr discs on a GALAXY series 5000 FT-IR spectrometer GL-7020. Electrospray experiments: Positive-ion electrospray mass spectrometry was performed using a Micromass model LCT TOF-MS with nitrogen as a

nebulization gas (Micromass Limited, Wythenshawe, Manchester, UK). UV spectra were measured using a Hewlett Packard HP8452A diode array spectrophotometer fitted with a 2 mm path-length quartz cell. Fluorescence spectra were determined using a Varian Cary Eclipse® fluorescence spectrophotometer operating Cary Eclipse® software. HPLC: Chromatography was performed using a system comprising a Perkin Elmer PE250 isocratic pump, PE ISS200 autosampler and PE 235C diode-array detector. Chromatograms were collected, stored and processed using the Labsystems Ltd X-Chrom® chromatography data system.

(±) *trans*-N,N^2-*bis*-7-(trifluoromethyl-quinolin-4-yl) cyclohexane-1,2-diamine 6-*trans*

Preparation using adaptation of a literature method[2a] produced a brown compound in quantitative yield. Suspension and vortexing in chloroform/ conc. NH_3 for one hour, filtering at the pump and washing with chloroform (5 x 25 ml) at the pump produced a tan solid)[2b]; free base: m.p. 350.8 °C, DSC scan: 25 to 400 °C at 5.0 °C min^{-1}). FT-IR cm^{-1}: 3436 (medium intensity, broadened N-H stretch); 1327 Amine γ (C-N) aromatic stretch.

(±) *trans*-N^1,N^2-*bis*-(2,8-*bis*-trifluoromethyl-quinolin-4-yl) cyclohexane-1,2-diamine. 7c-*trans*

After recrystallization (x3) from acetone/HCl the dihydrochloride was a gray solid: m.p. > 380 ^oC (decomposition). MS: (EI at 70 eV)) $C_{25}H_{20}N_4F_{12}$ 640 Da. Detected, 640 ($M^{+}\cdot$, 4 %), 360 ($M^{+}\cdot$ -F·,1 %), 360 (15 %), $CF3^+$, 69 (8 %), 319 (6 %), 307 (5 %), 280 (5 %), 36 (100 %). The dihydrochloride (100mg), was suspended in chloroform (100 ml) to which was added concentrated NH_3 (33 % solution in water, 100 ml) and stirred then left for one week. The solution slowly deposited a mass of clear crystals. These were isolated by filtration then

slowly crystallized by diffusion of methanol into chloroform. Free base: m.p. 243.4 –245.2 °C DSC: 0 ° C to 300 °C ramped at 10 °C min^{-1}).

^{1}H NMR: δ_H (300 MHz, DMSO-d_6, 25 ºC): δ = 1.49 (broad t, 2 H, $^{3}J_{\text{H ax-H ax}}$ = 9.48 Hz), 1.77-1.89 (m, 4H), 2.06 (d, 2H, $^{3}J_{\text{H ax-H ax}}$ = 12.64 Hz), 4.00 (m, 2H), 7.16 (s, 2H, H-3), 7.37 (t, 2H, H-6, $^{3}J_{\text{H-H}}$ = 7.92 Hz), 7.46 (broad d, 2 NH), 7.89 (d, H-5, 2H, $^{3}J_{\text{H-H}}$ = 7.20 Hz), 8.27 (d, $^{3}J_{\text{H-H}}$ = 8.49 Hz). Methanol peak at 3.33 ppm (24 H). ^{13}C NMR (75 MHz, 25 ºC, DMSO-d_6): δ = 24.6 (C-3 CH_2), 31.2 (C-2 CH_2), 56.8 (C-1 CH), 95.1 (C-3' CH), 123.7 (C-6' CH), 126.3 (C-5' CH), 128.5 (C-7' CH), 125.8 (C-8" quartet, $^{2}J_{\text{C-F}}$ = 29 Hz, 143.5 C-9' 4 °C), 147.3 (C-2" quartet, $^{2}J_{\text{C-F}}$ = 33 Hz), 152.0 (C-4 4 °C), 114.6-129.2 (2 distorted quartets, C-8', C-2', $^{2}J_{\text{C-F}}$ = ca. 114 and 110 Hz respectively). IR (Nujol) = 3436 (medium intensity, Sharp N-H stretch); 1315, 1292 cm^{-1} (strong 2° Amine γ (C-N), aromatic stretching vibration).

Similarly, compounds **5**, **6** and **7** were constructed according to published methods [2].

Crystallography

Crystal Data **7c**-*trans*, $C_{25}H_{20}F_{12}N_4O$, M = 620.46, triclinic, a = 11.026(4), b = 11.043(4), c = 12.808(4) Å, α = 93.963(4), β = 108.986(5), γ = 92.591(5)^{o}, U = 1467.3(9) $Å^3$, spacegroup P-1, d_{calc} = 1.404 gcm^{-3}, Z = 2. Data were measured with MoKα radiation using the MARresearch Image Plate System The crystal was positioned at 70 mm from the Image Plate. 100 frames were measured at 2^{o} intervals with a counting time of 2 mins. Data analysis was carried out with the XDS program [64] to provide 4816 independent reflections. The structure was solved using direct methods with the Shelx86 program. [65] Non-hydrogen atoms were refined with anisotropic thermal parameters. The hydrogen atoms bonded to carbon were included in geometric positions and given thermal parameters equivalent to 1.2

times those of the atom to which they were attached. The structure was refined on F^2 using Shelxl [66] to R1 0.0832, wR2 0.1226 for 1821 reflections respectively with $I>2\sigma(I)$. The data have been deposited at the Cambridge Crystallographic Data Centre with reference number CCDC 223083.

UV Spectroscopic studies

The UV spectra of the two compounds were determined over the range 190 – 800 nm on Thermo Scientific Evolution 300 spectrophotometer as described in the Supporting Information.

Mass spectrometric studies[23]

Samples were dissolved in a 1:1 (v/v) mixture of water and acetonitrile containing 0.1% v/v of formic acid and diluted so as to yield approximately 3 μg/ml solutions. These were then each infused into the mass spectrometer at a rate of 3 μl/min, using a 250 μl glass syringe fitted into a Harvard Apparatus Model II syringe driver. Spectra were collected at a rate of 1 per second over a three minute period. For accurate mass determinations, a reference solution containing 10 μg/ml of Leucine-Enkephalin in acetonitrile/water/formic acid was infused at a rate of 3 μl/min into the Lockspray™ attachment using a second syringe. The analyte and reference streams were sampled at a rate of one spectrum per second over a three-minute period and the spectra averaged. The MassLynx® software was used to adjust the average analyte spectrum on the basis of the observed base-peak mass of the average leucine-enkaphalin spectrum, which has a nominal mass of 556.2771 Da. Instrumental operating conditions were factory standard with the following variable settings: Capillary: 2250V; Sample cone: 30V; Extraction cone: 10V; RF Lens: 1000V; Desolvation gas flow:638 L/min; Desolvation temperature: 150º C; Source temperature: 100ºC.

High performance liquid chromatographic studies

Approximately 1.5 mg samples were shaken with 1.5 ml aliquots of the HPLC eluent and left to stand for several minutes before being centrifuged at 14,000 rpm for 1 min. A 1 ml aliquot of the supernatant was then *trans*ferred to a 2 ml autosampler vial, which was sealed and placed in the autosampler. The following instrumental conditions were employed: Eluent: 0.1M KH_2PO_4/0.1M $NaClO_4$ adjusted to pH 2.0 ($HClO_4$): Acetonitrile (87:13 $^{v}/_{v}$) Flow rate: 1.0 ml/min (approx. 1650 psi); Injection 10 µl; Column Phenomenex Lichrosphere 5CN, 4.6 x 150 mm; Detection 254 nm.

Antimalarial Efficacy [2]

P. berghei N/13 (2×10^7 parasitized erythrocytes) was inoculated intravenously (i.v.) in MF1 mice supplied by the Biological Services Unit, The University of Manchester, UK. Mice were housed in groups within plastic cages (length 38 cm × width 22 cm × height 11cm) at room temperature (19-22°C), on a 12h light (08:00-20:00) and 12h dark (20:00-08:00) cycle, with unlimited access to food (CRM feeding pellets, SDS) and water. Experiments were licensed under the Animals (Scientific Procedures) Act 1986. In compliance with the conditions of the licence, infected mice were humanely killed when humane endpoints were reached. Parasitaemia was measured by counting Leishman-positive cells 72 h following infection using tail blood smears stained with Leishman's reagent (Sigma Chemical Co., USA) 2 mg/ml methanol. Parasitaemia was calculated as the mean percentage (%) ± SEM of erythrocytes containing Leishman-positive bodies for groups of 4 – 8 mice for each dose tested. Drugs were delivered by the subcutaneous (s.c., 5 injections over 72 h), intraperitoneal (i.p., 5 injections over 72 h) as described previously.[10-11] An

appropriate number of dose levels (2-8) were investigated for each compound, in order to determine the dose of drug (ID_{50}) required to inhibit parasitaemia by 50% compared with parasitaemia in concurrent vehicle-treated mice. (±)-*trans*-N^1,N^2-*bis*-(7-chloroquinolin-4-yl)cyclohexane-1,2-diamine **5**-*trans* (ID_{50} = 3.0 mg/kg; 8.3mmol/kg) and the 7-trifluoromethyl analogue **6**-*trans*, (ID_{50} = 5.9 mg/kg; 14.9 mmol/kg) was active. However, the bistrifluoromethyl analog **7c**-*trans* was inactive *in vivo*: there was no reduction in parasitaemia following 5 x doses of 10 and 50 mg/kg, compare with treated with vehicle treated animals (control parasitaemia: 65 %) Chloroquine diphosphate **4a** was used as the control compound (ID_{50} = 4.3 mg/kg; 8.3 mmol/kg).

Acknowledgements

Giles C. Edwards and Margaret M. Hawkins provided expert technical assistance for DSC, NMR and HPLC-MS experiments. Dr Shaun Higgins is credited with expert assistance involving multi-dimensional NMR experiments. We thank EPSRC and the University of Reading for funds for the Image Plate system. The FT-NMR system and Accurate Mass spectrometer (LJMU) was purchased through a SRIF award from EPSRC and the Wellcome Trust. AJF thanks Bruker for funding. All EPR experiments were carried out at the EPSRC National EPR Service. VL acknowledges Early Stage Researcher funding from the European Union's Seventh Framework Programme FP7-PEOPLE-2013-ITN through the 'MAGnetic Innovation in Catalysis' (MAGIC) Initial Training Network (Grant agreement no. 606831). FC thanks the Conacyt Mexico for a studentship.

Dedication

This paper is dedicated to Joshua Lederberg for long discussions, mentorship, and above all friendship.

References

[1] M. M. van Riemsdijk, M. M. van der Klauw, K. J. A. C. van Heest, F. R. Reedeker, R. J. Ligthelm, R. M. C. Herings, B. H. C. Stricker, *Eur J Clin Pharmacol* **1997**, *52*, 1-6.

[2] a) F. M. D. Ismail, M. J. Dascombe, P. Carr, S. E. North, *J Pharm Pharmacol* **1996**, *48*, 841-850; b) F. M. D. Ismail, M. J. Dascombe, P. Carr, S. A. M. Merette, P. Rouault, *J Pharm Pharmacol* **1998**, *50*, 483-492.

[3] a) T. Gabay, M. Krugliak, G. Shalmiev, H. Ginsburg, *Parasitology* **1994**, *108*, 371-381; b) T. J. Egan, W. W. Mavuso, D. C. Ross, H. M. Marques, *J Inorg Biochem* **1997**, *68*, 137-145; c) A. C. Chou, R. Chevli, C. D. Fitch, *Biochemistry-Us* **1980**, *19*, 1543-1549.

[4] a) K. Nakatani, H. Ishikawa, S. Aono, Y. Mizutani, *Sci Rep-Uk* **2014**, *4*, 6137; b) L. M. Coronado, C. T. Nadovich, C. Spadafora, *Bba-Gen Subjects* **2014**, *1840*, 2032-2041.

[5] a) S. Pagola, P. W. Stephens, D. S. Bohle, A. D. Kosar, S. K. Madsen, *Nature* **2000**, *404*, 307-310; b) M. A. Ambele, B. T. Sewell, F. R. Cummings, P. J. Smith, T. J. Egan, *Crystal Growth & Design* **2013**, *13*, 4442-4452.

[6] C. Tempera, R. Franco, C. Caro, V. Andre, P. Eaton, P. Burke, T. Hanscheid, *Malaria J* **2015**, *14*.

[7] F. M. D. Ismail, *J Fluorine Chem* **2002**, *118*, 27-33.

[8] D. C. Hooper, *Quinolone Antimicrobial Agents Vol. 2nd edition* American Society for Microbiology, Washington, **1993**.

[9] E. P. Gillis, K. J. Eastman, M. D. Hill, D. J. Donnelly, N. A. Meanwell, *J Med Chem* **2015**, *58*, 8315-8359.

[10] M. L. Pacholski, N. Winograd, *Chem Rev* **1999**, *99*, 2977-3005.

[11] J. L. Guerquin-Kern, M. Coppey, D. Carrez, A. C. Brunet, C. H. Nguyen, C. Rivalle, G. Slodzian, A. Croisy, *Microsc Res Techniq* **1997**, *36*, 287-295.

[12] H. Andersag, S. Breitner, H. Jung, I. G. Farbenind, German Patent: DE683692, Germany, **1937**.

[13] D. Y. D. De, F. M. Krogstad, L. D. Byers, D. J. Krogstad, *J Med Chem* **1998**, *41*, 4918-4926.

[14] A. Sveinbjornsson, C. A. Vanderwerf, *J Am Chem Soc* **1951**, *73*, 1378-1379.

[15] B. K. Park, O'Neill, P. M., Ward, S. A., Stocks, P. A., Anti-Malarial Compounds, Patent number: PCT/GB02/01410, **2002**.

[16] D. De, Krogstad, F.M., Byres, L.D., Krogstad, D.J., *J Med Chem* **1998**, *41*, 4918-4926.

[17] J. A. McIntyre, Castaner, J., Bayes, M., *Drugs of the future* **2003**, *28*, 859-869.

[18] a) P. Lim, *Analytical profiles of drug substances* **1985**, *14*, 157-180; b) D. F. Clyde, V. C. Mccarthy, C. C. Rebert, R. M. Miller, *Antimicrob Agents Ch* **1973**, *3*, 220-223; c) C. J. Ohnmacht, A. R. Patel, R. E. Lutz, *J Med Chem* **1971**, *14*, 926-928; d) G. M. Trenholme, R. L. Williams, R. E. Desjardins, H. Frischer, P. E. Carson, K. H. Rieckmann, C. J. Canfield, *Science* **1975**, *190*, 792-794; e) S. Kitchener, *ADF Health* **2003**, *4*, 34-38; f) F. Y. Wiselogle, *A Survey of Antimalarial Drugs, 1941 - 1945*, Edwards, Ann Arbor, Michigan, **1946**; g) A. G. Craig, G. E. Grau, C. Janse, J. W. Kazura, D. Milner, J. W. Barnwell, G. Turner, J. Langhorne, H. R. M. A. Model, *Plos Pathog* **2012**, *8*; h) T. N. Pullman, L. Eichelberger, A. S. Alving, R. Jones, B. Craige, C. M. Whorton, *J Clin Invest* **1948**, *27*, 12-16.

[19] a) R. A. Mirghani, U. Yasar, T. Zheng, J. M. Cook, L. L. Gustafsson, G. Tybring, O. Ericsson, *Drug Metab Dispos* **2002**, *30*, 1368-1371; b) P. V. V. S. Sarma, D. M. Han, J. R. Deschamps, J. M. Cook, *J Nat Prod* **2005**, *68*, 942-944.
[20] C. H. Kaschula, T. J. Egan, R. Hunter, N. Basilico, S. Parapini, D. Taramelli, E. Pasini, D. Monti, *J Med Chem* **2002**, *45*, 3531-3539.
[21] D. Kuter, V. Streltsov, N. Davydova, G. A. Venter, K. J. Naidoo, T. J. Egan, *J Inorg Biochem* **2016**, *154*, 114-125.
[22] F. M. D. Ismail, M. G. B. Drew, M. J. Dascombe, *Chimica Oggi - Chemistry Today* **2009**, *27*, 16-20.
[23] M. J. Dascombe, M. G. B. Drew, H. Morris, P. Wilairat, S. Auparakkitanon, W. A. Moule, S. Alizadeh-Shekalgourabi, P. G. Evans, M. Lloyd, A. M. Dyas, P. Carr, F. M. D. Ismail, *J Med Chem* **2005**, *48*, 5423-5436.
[24] A. Haberkorn, H. P. Kraft, G. Blaschke, *Tropenmed Parasitol* **1979**, *30*, 308-312.
[25] a) P. C. Lima, M. A. Avery, B. L. Tekwani, H. D. Alves, E. J. Barreiro, C. A. M. Fraga, *Farmaco* **2002**, *57*, 825-832; b) Y. T. Pham, F. Nosten, R. Farinotti, N. J. White, F. Gimenez, *Int J Clin Pharm Th* **1999**, *37*, 58-61; c) H. Tajerzadeh, D. J. Cutler, *Biopharm Drug Dispos* **1993**, *14*, 87-91.
[26] F. M. D. Ismail, P. Carr, S. Alizadeh-Shekalgourabi, S. Alizadeh-Shekalgourabi, P. G. Evans, W. A. Moule, S. North, P. Wilairat, S. Auparakkitanon, M. J. Dascombe, **A**bstracts presented at: Gordon Research Conference, Malaria, Somerville College Oxford, United Kingdom, July 26-31, 1998; https://www.grc.org/programs.aspx?id=4556; See Figure S18.
[27] E. A. Robinson, S. A. Johnson, T. H. Tang, R. J. Gillespie, *Inorg Chem* **1997**, *36*, 3022-3030.
[28] H. L. Yale, *J Med Pharmaceut Ch* **1959**, *1*, 121-133.
[29] M. J. Dascombe, M. G. B. Drew, P. G. Evans, F. M. D. Ismail, *Frontiers in Drug Design and Discovery* **2007**, *3*, 559-609.
[30] *Benzimidazoles and Cogeneric Tricyclic Compounds, Part 2 (The Chemistry of Heterocyclic Compounds, Vol. 40*, (Ed. P. N. Preston, M. F. G. Stevens, G. Tennant), Wily, 1981.
[31] Y. B. Vysotskii, V. A. Sokolenko, *J Appl. Spectrosc.* **1980**, *32*, 398-403.
[32] T. Ganguly, S. B. Banerjee, *Can J Chem* **1982**, *60*, 741-746.
[33] H. Andersag, S. Breitner, H. Jung, German patent: 683, 692, Germany, **1939**.
[34] a) G. B. Barlin, T. M. T. Nguyen, B. Kotecka, K. H. Rieckmann, *Aust J Chem* **1993**, *46*, 21-29; b) G. B. Barlin, S. J. Ireland, C. Jiravinyu, T. M. T. Nguyen, B. Kotecka, K. H. Rieckmann, *Aust J Chem* **1993**, *46*, 1695-1703; c) J. Elbenna, J. Hakim, M. T. Labro, *Biochem Pharmacol* **1992**, *43*, 527-532; d) I. M. Kapetanovic, J. H. Digiovanni, J. F. Bartosevich, V. Melendez, A. C. Schroeder, J. Vonbredow, M. H. Heiffer, *J Chromatogr-Biomed* **1987**, *419*, 458-463; e) G. B. Barlin, S. J. Ireland, T. M. T. Nguyen, B. Kotecka, K. H. Rieckmann, *Aust J Chem* **1994**, *47*, 1553-1560; f) G. B. Barlin, S. J. Ireland, T. M. T. Nguyen, B. Kotecka, K. H. Rieckmann, *Aust J Chem* **1993**, *46*, 1685-1693; g) G. B. Barlin, F. L. Tian, B. Kotecka, K. H. Rieckmann, *Aust J Chem* **1992**, *45*, 1845-1855; h) G. B. Barlin, T. M. T. Nguyen, B. Kotecka, K. H. Rieckmann, *Aust J Chem* **1992**, *45*, 1651-1662; i) G. B. Barlin, C. Jiravinyu, G. A. Butcher, B. Kotecka, K. Rieckmann, *Ann Trop Med Parasit* **1992**, *86*, 323-331; j) G. B. Barlin, W. L. Tan, *Aust J Chem* **1985**, *38*, 1827-1835; k) G. B. Barlin, C. Jiravinyu, *Aust J Chem* **1991**, *44*, 151-156; l) S. R. Hawley, P. G. Bray, P. M. ONeill, D. J. Naisbitt, B. K. Park, S. A. Ward, *Antimicrob Agents Ch* **1996**, *40*, 2345-2349; m) J. E. Ruscoe, H. Jewell, J. L. Maggs, P. M. Oneill, R. C. Storr, S. A. Ward, B. K. Park, *J Pharmacol Exp Ther* **1995**, *273*, 393-404; n) P. A. Stocks, K. J.

Raynes, P. G. Bray, B. K. Park, P. M. O'Neill, S. A. Ward, *J Med Chem* **2002**, *45*, 4975-4983; o) J. Adovelande, Y. Boulard, J. P. Berry, P. Galle, G. Slodzian, J. Schrevel, *Biol Cell* **1994**, *81*, 185-192.
[35] J. M. Karle, I. L. Karle, *Acta Crystallogr C* **1991**, *47*, 2391-2395.
[36] J. M. Karle, I. L. Karle, *Antimicrob Agents Chemother* **2002**, *46*, 1529-1534.
[37] Accelrys, Inc., Cerius2 Modeling Environment, Release 4.8, San Diego: Accelrys Software Inc., **2005**.
[38] Gaussian 09, Revision A.01, M. J. Frisch, G. W. Trucks, H. B. Schlegel, G. E. Scuseria, M. A. Robb, J. R. Cheeseman, G. Scalmani, V. Barone, G. A. Petersson, H. Nakatsuji, X. Li, M. Caricato, A. Marenich, J. Bloino, B. G. Janesko, R. Gomperts, B. Mennucci, H. P. Hratchian, J. V. Ortiz, A. F. Izmaylov, J. L. Sonnenberg, D. Williams-Young, F. Ding, F. Lipparini, F. Egidi, J. Goings, B. Peng, A. Petrone, T. Henderson, D. Ranasinghe, V. G. Zakrzewski, J. Gao, N. Rega, G. Zheng, W. Liang, M. Hada, M. Ehara, K. Toyota, R. Fukuda, J. Hasegawa, M. Ishida, T. Nakajima, Y. Honda, O. Kitao, H. Nakai, T. Vreven, K. Throssell, J. A. Montgomery, Jr., J. E. Peralta, F. Ogliaro, M. Bearpark, J. J. Heyd, E. Brothers, K. N. Kudin, V. N. Staroverov, T. Keith, R. Kobayashi, J. Normand, K. Raghavachari, A. Rendell, J. C. Burant, S. S. Iyengar, J. Tomasi, M. Cossi, J. M. Millam, M. Klene, C. Adamo, R. Cammi, J. W. Ochterski, R. L. Martin, K. Morokuma, O. Farkas, J. B. Foresman, and D. J. Fox, Gaussian, Inc., Wallingford CT, **2016**.
[39] B. Kuhn, P. Mohr, M. Stahl, *J Med Chem* **2010**, *53*, 2601-2611.
[40] J. M. Karle, A. K. Bhattacharjee, J. L. Vennerstrom, *J Chem Crystallogr* **2002**, *32*, 133-139.
[41] S. Miertus, J. Tomasi, *Chem Phys* **1982**, *65*, 239-245.
[42] R. Salvio, M. Moliterno, D. Caramelli, L. Pisciottani, A. Antenucci, M. D'Amico, M. Bella, *Catal Sci Technol* **2016**, *6*, 2280-2288.
[43] F. H. Allen, O. Kennard, D. G. Watson, L. Brammer, A. G. Orpen, R. Taylor, *J Chem Soc Perk T 2* **1987**, S1-S19.
[44] S. Furuseth, J. Karlsen, A. Mostad, C. Romming, R. Salmen, H. H. Tonnesen, *Acta Chem Scand* **1990**, *44*, 741-745.
[45] V. Ferrari, D. J. Cutler, *J Pharm Sci* **1987**, *76*, 554-556.
[46] V. R. Solomon, H. Lee, *Eur J Pharmacol* **2009**, *625*, 220-233.
[47] *Ernst Schering Research Foundation Workshop: Computer Aided Drug Design in Industrial Research, Vol. 15*, Springer, **1995**.
[48] a) A. S. Paul, S. Saha, K. Engelberg, R. H. Y. Jiang, B. I. Coleman, A. L. Kosber, C. T. Chen, M. Ganter, N. Espy, T. W. Gilberger, M. J. Gubbels, M. T. Duraisingh, *Cell Host Microbe* **2015**, *18*, 49-60; b) D. J. Sullivan, I. Y. Gluzman, D. G. Russell, D. E. Goldberg, *P Natl Acad Sci USA* **1996**, *93*, 11865-11870.
[49] a) W. Devine, J. L. Woodring, U. Swaminathan, E. Amata, G. Patel, J. Erath, N. E. Roncal, P. J. Lee, S. E. Leed, A. Rodriguez, K. Mensa-Wilmot, R. J. Sciotti, M. P. Pollastri, *J Med Chem* **2015**, *58*, 5522-5537; b) W. C. Van Voorhis, J. H. Adams, R. Adelfio, V. Ahyong, M. H. Akabas, P. Alano, A. Alday, Y. A. Resto, A. Alsibaee, A. Alzualde, K. T. Andrews, S. V. Avery, V. M. Avery, L. Ayong, M. Baker, S. Baker, C. Ben Mamoun, S. Bhatia, Q. Bickle, L. Bounaadja, T. Bowling, J. Bosch, L. E. Boucher, F. F. Boyom, J. Brea, M. Brennan, A. Burton, C. R. Caffrey, G. Camarda, M. Carrasquilla, D. Carter, M. B. Cassera, K. C. C. Cheng, W. Chindaudomsate, A. Chubb, B. L. Colon, D. D. Colon-Lopez, Y. Corbett, G. J. Crowther, N. Cowan, S. D'Alessandro, N. Le Dang, M. Delves, J. L. DeRisi, A. Y. Du, S. Duffy, S. A. El-Sayed, M. T. Ferdig, J. A. F. Robledo, D. A. Fidock, I. Florent, P. V. T. Fokou, A. Galstian, F. J. Gamo, S. Gokool, B. Gold, T. Golub, G. M. Goldgof, R. Guha, W. A.

Guiguemde, N. Gural, R. K. Guy, M. A. E. Hansen, K. K. Hanson, A. Hemphill, R. H. van Huijsduijnen, T. Horii, P. Horrocks, T. B. Hughes, C. Huston, I. Igarashi, K. Ingram-Sieber, M. A. Itoe, A. Jadhav, A. N. Jensen, L. T. Jensen, R. H. Y. Jiang, A. Kaiser, J. Keiser, T. Ketas, S. Kicka, S. Kim, K. Kirk, V. P. Kumar, D. E. Kyle, M. J. Lafuente, S. Landfear, N. Lee, S. Lee, A. M. Lehane, F. W. Li, D. Little, L. Q. Liu, M. Llinas, M. I. Loza, A. Lubar, L. Lucantoni, I. Lucet, L. Maes, D. Mancama, et al., *Plos Pathog* **2016**, *12*.

[50] G. C. Terstappen, C. Schlupen, R. Raggiaschi, G. Gaviraghi, *Nat Rev Drug Discov* **2007**, *6*, 891-903.

[51] D. Jani, R. Nagarkatti, W. Beatty, R. Angel, C. Slebodnick, J. Andersen, S. Kumar, D. Rathore, *Plos Pathog* **2008**, *4*.

[52] F. M. D. Ismail, M. G. B. Drew, M. J. Dascombe, I. P. Clark, A. W. Parker, in *CCLRC Annual Report*, Central Laser Facility, **2004**, pp. 119-120.

[53] a) M. A. Sainna, S. Kumar, D. Kumar, S. Fornarini, M. E. Crestoni, S. P. de Visser, *Chem Sci* **2015**, *6*, 1516-1529; b) F. G. C. Reinhard, M. A. Sainna, P. Upadhyay, G. A. Balan, D. Kumar, S. Fornarini, M. E. Crestoni, S. P. de Visser, *Chem-Eur J* **2016**, *22*, 18608-18619.

[54] a) A. D. Becke, *J Chem Phys* **1993**, *98*, 5648-5652; b) C. T. Lee, W. T. Yang, R. G. Parr, *Phys Rev B* **1988**, *37*, 785-789.

[55] P. J. Hay, W. R. Wadt, *J Chem Phys* **1985**, *82*, 270-283.

[56] a) D. F. Koenig, *Acta Crystallogr* **1965**, *18*, 663-673; b) J. Gildenhuys, T. le Roex, T. J. Egan, K. A. de Villiers, *J Am Chem Soc* **2013**, *135*, 1037-1047; c) J. Gildenhuys, R. Müller, T. le Roex, K. A. de Villiers, *Solid State Sciences* **2017**, *in press*.

[57] K. A. de Villiers, H. M. Marques, T. J. Egan, *J Inorg Biochem* **2008**, *102*, 1660-1667.

[58] K. A. de Villiers, J. Gildenhuys, T. le Roex, *Acs Chem Biol* **2012**, *7*, 666-671.

[59] J. Gildenhuys, C. J. Sammy, R. Muller, V. A. Streltsov, T. le Roex, D. Kuter, K. A. de Villiers, *Dalton T* **2015**, *44*, 16767-16777.

[60] A. P. Gorka, A. de Dios, P. D. Roepe, *J Med Chem* **2013**, *56*, 5231-5246.

[61] G. Macetti, L. Loconte, S. Rizzato, C. Gatti, L. Lo Presti, *Cryst Growth Des* **2016**, *16*, 6043-6054.

[62] F. M. D. Ismail, A. H. Cox, N. M. Dempster, J. L. Ford, M. J. Dascombe, M. G. B. Drew, *J Pharm Pharmacol* **2010**, *62*, 1489-1490.

[63] E. L. Dodd, D. S. Bohle, *Chem Commun* **2014**, *50*, 13765-13768.

[64] M. S. Walczak, K. Lawniczak-Jablonska, A. Wolska, M. Sikora, A. Sienkiewicz, L. Suarez, A. J. Kosar, M. J. Bellemare, D. S. Bohle, *J Phys Chem B* **2011**, *115*, 4419-4426.

[65] F. M. D. Ismail, H. Morris, N. M. Dempster, I. Y. Saleem, I. Y. Kasaija, H. V. Truong, L. E. Randle, S. Alizadeh-Shekalgourabi, E. G., J. P. Williams, M. J. Dascombe, M. G. B. Drew, in *From Atoms to Biomolecules: Celebrating the technological innovations in mass spectrometry on the 30th Anniversary of Fast Atom Bombardment (FAB)*, Cardiff City Hall, Cardiff, **2011**.

[66] S. R. Meshnick, *Ann. Trop. Med. Parasitol.* **1996**, *90*, 367-372.

[67] a) I. Constantinidis, Satterlee, J.D., *J. Am. Chem. Soc.* **1988**, *110*, 4391-4395; b) M. J. Dascombe, M. D. G. Drew, E. F.G., F. M. D. Ismail, in *Frontiers in drug design and discovery: Structure-based drug design in the 21st century, Vol. 3*, Bentham Science Publishers, **2007**, pp. 559-609.

[68] A. C. C. de Sousa, G. M. Viana, N. C. Diaz, M. G. Rezende, F. F. de Oliveira, R. P. Nunes, M. F. Pereira, A. L. L. Areas, M. G. Zalis, V. D. Frutuoso, H. C. D. Faria, T. F. S. Domingos, M. de Padula, L. M. Cabral, C. R. Rodrigues, *Chem Pharm Bull* **2016**, *64*, 594-601.